UNIVERSITY WEST

Fachhochschule Kaiserslautern | University of Applied Sciences

The performance of an iced aircraft wing

Daniel Andersson

2011-08-26

Bachelor´s thesis
Product development with design
Department of Engineering Science, University West

BACHELOR'S THESIS

The performance of an iced aircraft wing

Summary

The goal of this thesis work has been to develop and manufacture an ice layer which was to be mounted on the tip of a scaled down wing model. The iced wing should be tested in a wind tunnel and aerodynamic comparisons should be made to the same wing without ice.

The development of the ice was carried out as a modified product development process. The main differences are that there is no costumer and that the actual shape and functions of the product are more or less predetermined. The challenge was to find the best way to create the ice layer and how to mount it to the wing without damaging it or covering any pressure sensors. Product development methods such as pros and cons lists and prototypes were used to solve problems before printing the plastic ice layer in a rapid prototyping machine.

Wind tunnel experiments were then conducted on the wing with and without the manufactured ice. Raw data from the wind tunnel were processed and lift and drag coefficients were calculated using mathematical equations. Finally, conclusions were drawn by comparing the results from the wind tunnel tests with theory, other works as well as CFD simulations.

The ice layer was successfully manufactured and it met the target specifications. The aerodynamic performance of an iced aircraft wing proved to be considerably worse compared to a blank wing. The maximum achievable lift force decreased by 22% and an increased drag force will require more thrust from the airplane.

Date:	August 26, 2011
Author:	Daniel Andersson
Examiner:	Mats Eriksson (University West)
Advisor:	Prof. Dr.-Ing Norbert Gilbert, Prof. Dr.-Ing Karl-Heinz Helmstädter (University of Applied Sciences, Kaiserslautern) and Dr. Claes Fredriksson (University West)
Programme:	Product development with design
Main field of study:	Mechanical Engineering **Education level**: first cycle
Credits:	15 ECTS
Keywords	Airfoil, ice layer, in-flight icing, wind tunnel, rapid prototyping, lift force
Publisher:	University West, Department of Engineering Science, S-461 86 Trollhättan, SWEDEN Phone: + 46 520 22 30 00 Fax: + 46 520 22 32 99 Web: www.hv.se

Preface

This bachelor project work was completed at the University of Applied Sciences in Kaiserslautern, Germany starting early March 2011 and ending early August the same year. The thesis was carried out in parallel to a Master course (of 10 ECTS) and thus corresponds to 20 ECTS in the German curriculum.

The work was mainly conducted at the flow laboratory (strömungslabor) where flow experiments are performed and where the wind tunnel is placed. The parts for the ice layer and other prototypes were made using the rapid prototyping machine placed in a different building. I would like to thank Mrs Müller, Mr Girichidis and Mr Helmstädter for the assistance in handling this machine and I would also like to thank the staff at the workshop that helped me adjust the manufactured parts and the wing as well as lending me tools and equipment. Special thanks go to my supervisor Mr Gilbert as well as his assistant, Mr Niebergall who helped me greatly throughout the entire project. From University West I would like to thank Mrs Munkenberg, Mr Eriksson and Mr Fredriksson for their visit to Kaiserslautern and their useful comments regarding this report.

Finally I would like to thank Mr Meij for accepting me to the university and granting me the opportunity to do my thesis work abroad and gaining a very valuable experience. I have found my stay here rewarding and fun and I can recommend anyone to study abroad when presented with the opportunity.

Kaiserslautern, August 2011

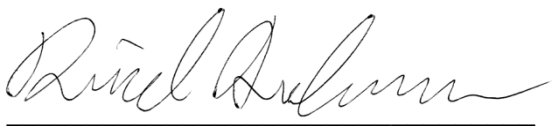

Daniel Andersson

Contents

Summary ii

Preface iii

Symbols and glossary vi

1 Introduction 1

1.1 Overview of previous work 1

1.2 Objectives 2

1.3 Limitations and assumptions 2

2 Theory 3

2.1 Pressure 3

2.2 Basic aerodynamics 4

2.3 In-flight icing 7

3 Equipment and software description 9

3.1 Wing replica 9

3.2 Rapid prototyping machine 9

3.3 Wind tunnel 10

3.4 Engauge digitizer 11

4 Methodology 12

4.1 Target specifications 13

4.2 Prototype creation 13

4.3 Solution generation 13

4.4 Choosing solutions 14

4.5 Implementation of solutions 15

4.6 Wind tunnel tests 15

4.7 Ansys Fluent 21

5 Ice layer development process 23

5.1 Ice layer specifications 23

5.2 The first prototype 23

5.3 Clarifying problems....26
5.4 Solutions....27
5.5 Implementing solutions....30
6 Wind tunnel test results and discussion....32
6.1 Lift force....32
6.2 Drag force....44
6.3 Velocity, pressure and density studies....50
7 Conclusions....52
7.1 Reflections....53
7.2 Future work....54
8 Bibliography....55

Appendix

Pros and Cons lists and Concept Scoring Matrix

Symbols and glossary

Airfoil	The profile of a wing
Angle of Attack	The angle between the chord of the wing and incoming flow of air
CFD	Computational Fluid Dynamics
Chord	The imaginary straight line from the leading edge to the trailing edge
Engauge Digitizer	Software converting an image into numbers [1]. For description, see chapter 3.4
Fluent	A CFD software from Ansys [2]
Free stream	The stream of fluid which is unaffected by any obstacles. Variables measured in the free stream are denoted with ∞
Leading edge	The front most section of the airfoil
LEWICE	2D ice accretion tool developed by NASA [3]
NWT	Near Wall Treatment, a setting in Fluent
Pro/Engineer	CAD tool from PTC [4]
RPM	Rapid Prototyping Machine (same as a 3D printer).
Stagnation point	The point on the airfoil which the incoming air first hits
Stalling	When the lift force decreases as the angle of attack increases. Starts occurring at the stall angle
Trailing edge	The edge at the end of the airfoil
C	Spring constant
C_L	Lift coefficient
C_D	Drag coefficient
C_P	Pressure coefficient, see chapter 2.1 for definition
α	Angle of attack [°]
P	Pressure [Pa] or [N/m^2]
ρ	Density [kg/m^3]
v	Velocity [m/s]
g	Force of gravity [m/s^2]
h	Elevation [m]
F_L	Lift Force [N]
F_D	Drag Force [N]
c	Chord length [0.162 m]
w	Wing width [0.5052 m]

1 Introduction

This thesis project was carried out at the University of Applied Sciences in Kaiserslautern, Germany. The main purpose of the work was to elucidate the aerodynamic effects of an iced airplane wing and make comparisons to a non-iced wing.

Aircraft icing is a threat to the security of aviation. De-icing with sprayed liquids is normally used in case of ground icing but is not possible during flight. The methods used in-flight today are either to heat the airfoil or to remove the ice using pneumatics via deformable surfaces. Not much is known about the influence of the many parameters in the icing process which has been a research theme at the University of Applied Sciences, Kaiserslautern during the past years.

1.1 Overview of previous work

Much work has already been done in the field of in-flight icing and the effect of iced wings. A summary of the work done in aircraft icing from the 30´s until present as well as the definitions of the four types of ice and their effect on the aerodynamic performance has been provided, for example by M.B. Brag *et al.* [5].

Previous wind tunnel experiments have also been carried out with iced wings to determine the effect of the ice. One such study conducted tests on the four types of ice with variations in roughness and position and compared the results with theory and ice accretion simulation models [6].

The most commonly used simulation model to simulate ice shapes on an airplane wing is NASA´s LEWICE ice accretion model [3]. This model evaluates the thermodynamics of the freezing process which occurs when super cooled droplets hit an airplane wing and generates the shape of the created ice layer. The input parameters for this model are pressure, velocity, droplet diameter, relative humidity and the meteorological parameters of liquid water [7]. These are temperature, relative humidity, precipitation, wind velocity, wind direction and solar radiation [8].

The wing replica used for this project was previously made by another student at the university.

Current work in progress at the university is the development of an aircraft icing code which is based on standard CFD tools like Ansys-Fluent/Open FOAM or engineering tools like Matlab. The purpose is to create a method which may be used

by aerodynamic engineers, enabling them to incorporate icing investigations in their work.

1.2 Objectives

The main goal of this thesis has been to create a plastic ice layer, mount it onto a scaled down airplane wing and perform tests in a wind tunnel. The shape of the ice layer is determined by a previous numeric simulation and it is created using a rapid prototyping machine in a number of parts which need to be assembled. The finished ice layer is mounted onto the scaled down wing with care taken not to damage the surface and to make sure that its pressure sensors are still functional, giving unbiased readings. When applied, tests on the drag, lift and pressure distribution over the wing are done which are compared to theoretical results, results from Fluent simulations as well as tests from a non-iced wing. The final goals are to describe and explain the findings and draw conclusions.

1.3 Limitations and assumptions

These are the limitations and assumptions for this thesis project:

- The ice shape is considered to have no gradients along the width of the wing. In reality, this is obviously not the case, but to generate such an ice layer would require skills and time which are not available.
- The ice is attached to a wing replica which is of a 1:10 scale of a real airplane wing. It is assumed that this downscaled wing gives satisfactory results.
- It is assumed that the shape of the first ice layer has been simulated in a correct way and that it corresponds well enough to reality.
- Because of time constrains, only one type of ice is created and tested.
- Constant temperature and wind velocity from the wind tunnel are presumed during the wind tunnel tests.
- No actions are taken to get the correct roughness of the ice surface.

2 Theory

This chapter provides a basic background on the aerodynamics of an airfoil, in-flight icing, pressure and flow separation. These aspects are vital in understanding the rest of the report.

2.1 Pressure

Assuming incompressible flow and thus constant density, the Bernoulli equation states that [9]:

$$P_{static} + \frac{\rho}{2} v^2 = P_{tot} = constant [eq. 1]$$

(The notation is explained in the glossary)

Or in words:

Static Pressure + Dynamic Pressure = Total Pressure

The total pressure remains constant along any streamline while the static and dynamic pressure may vary. Static pressure is the normal pressure which can be measured for every point in a flow field and is equal to a force per area. The dynamic pressure is related to the velocity of the fluid and is defined as the density times velocity squared divided by two. A high velocity results in a high dynamic pressure and vice versa. By assuming a constant total pressure, that also means that a *high* velocity results in a *low* static pressure.

Throughout this report, pressure is normalized into a pressure coefficient, C_p, defined as [10]:

$$C_p = \frac{P - P_\infty}{\frac{\rho_\infty}{2} v_\infty^2} \ [eq. 2]$$

Where P equals to the pressure at the point being evaluated and where variables denoted with a "∞" is the corresponding values in the free stream. The free stream is defined as the stream of fluid which is unaffected by any obstacles. Total, static and dynamic pressure may be normalized into a pressure coefficient.

2.2 Basic aerodynamics

This part summarizes the basic theory behind aerodynamic effects of an airfoil and how lift is generated and calculated. Figure 1 explains the terminology of an airfoil.

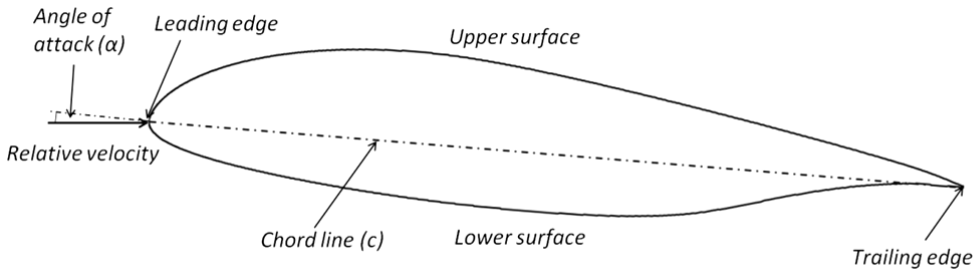

Figure 1 – The terminology of an airfoil

The forces acting on an airfoil are the gravity, thrust lift force and drag force. Gravity is always directed towards the ground. Thrust is the force produced by the airplane engine and is directed forward in regard to the airplane. The lift force is the force generated by the wings and is directed perpendicular to the relative wind. The drag force is the force opposing the aircraft's motion through the air and is directed parallel to the relative wind.

2.2.1 Lift force

The most common and most widely spread explanation on how lift is generated on an airfoil is based on the Bernoulli effect.

As previously explained, if the velocity increases the static pressure must decrease and vice versa to keep equation 1 valid. For positive angles of attack, the geometry of an airfoil forces the air at the upper surface to travel at higher velocities compared to the wind at the lower surface. This will, according to Bernoulli's equation, generate a low pressure at the upper surface and a high pressure at the lower surface, causing a lift force.

This theory is easy to understand but is *not* the full explanation. This can easily be realized by the fact that an acrobatic airplane is able to fly upside down. If the lift force was only due to the Bernoulli effect, the lift vector would point towards the ground in an upside down flight and thus causing the plane to fall to the ground.

To explain the lift force further, Newton's third law of motion is applied. It states that for every force in nature there is always an equal reaction force, acting in the opposite direction. By observing the airflow on an airfoil, we see that it is steered downward after the wing, causing a so called downwash. When the air is forced down, a

downward momentum is given to it which in turn creates an upward momentum on the airfoil, causing a lift force. See Figure 2.

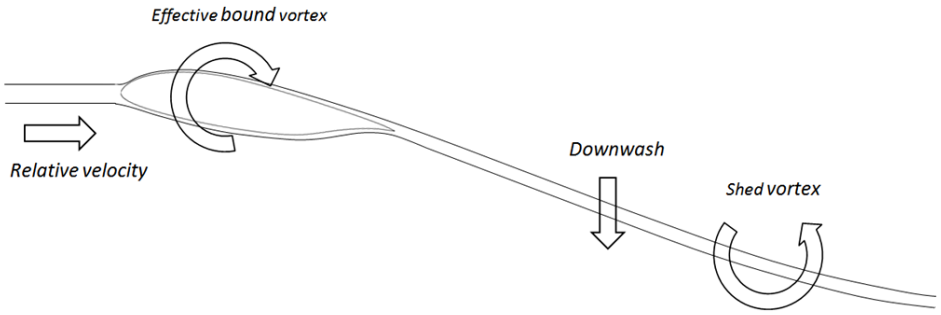

Figure 2 – Illustration showing the downwash and the resulting momentum

Hence, the lift force is a combination of Bernoulli's effect, which causes a lower pressure at the upper surface, and Newton´s third law which causes an upward momentum on the wing because of the downwash generated by the wing [11].

The lift force may be calculated by using the following equation [9]:

$$F_L = \frac{\rho}{2} v^2 c w C_L \; [eq.3]$$

By studying equation 3, one can see that the velocity has the biggest impact on the lift force. This explains why airplanes need a higher angle of attack at low velocities to maintain the lift force.

The lift coefficient, C_L, is a dimensionless number which describes an airfoils aerodynamic lift characteristics. The lift coefficient is mainly determined by the shape of the airfoil and the angle of attack. There is no simple way to calculate the lift coefficient since the shape of an airfoil is not easily defined. The best way to calculate the lift coefficient is by measuring it in a wind tunnel. Generally, as the angle of attack increases, the lift coefficient also increases.

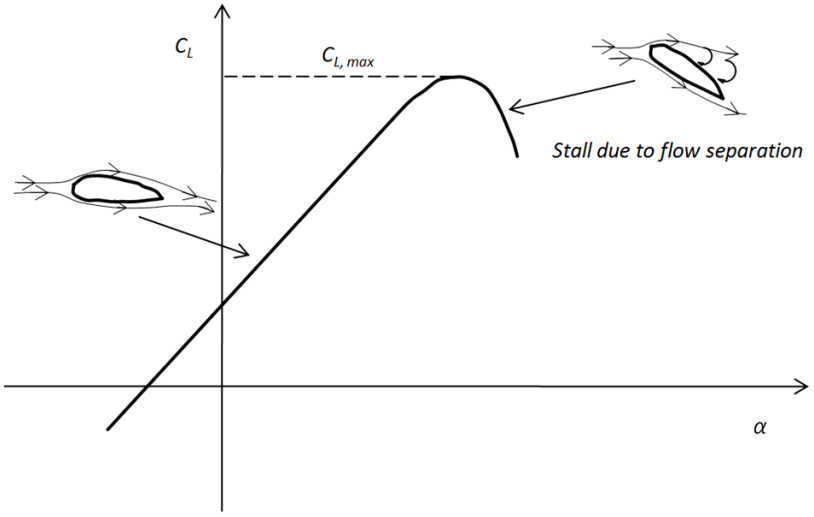

Figure 3 – Graph illustrating the lift-coefficient variation with the angle of attack

At low to medium angles of attack, the lift coefficient varies linearly with α, as can be seen in Figure 3. In this region, the airflow follows the airfoils curvature and is attached to its surface. The maximum lift coefficient is denoted $C_{L,\,max}$ and occurs just before the airfoil starts stalling. The maximum lift coefficient is one of the most important aspects of the aerodynamic performance of an airfoil, since it decides the point where it's no longer possible to increase C_L [10]. After this point, the airfoil will begin to stall and the forces required to bend, or "steer" the air, are greater than the viscosity of the air can support. This will result in a separation of flows and the air on the upper surface will break free and thus reducing the lift force considerably.

2.2.2 Drag force

Drag is a mechanical force which is generated when a solid body is moving through a fluid. The drag is described as the difference in velocity between the fluid and the body, if there is no difference in velocity there is no drag force. There are many factors that affect the magnitude of the drag force. One such factor is the so called skin friction. This is basically an aerodynamic friction between the surface of the wing and the air molecules. Another factor is the form drag which depends on the shape of the airfoil. The last main factor is the induced drag. This is caused by swirling flows at the wingtips which arise because of the pressure difference between the upper and lower surfaces. The induced drag can be reduced by using so called winglets at the wingtips.

The drag force may be calculated using the following equation [9]:

$$F_D = \frac{\rho}{2} v^2 c w C_D \; [eq.4]$$

The drag coefficient is, just as the lift coefficient, hard to calculate and is also mainly determined by the shape of the airfoil and the angle of attack.

2.3 In-flight icing

Icing on airplanes occurs while flying through humid clouds at sub-zero temperatures. When ice is accreted on the wings of an airplane, it will result in an increase in drag force and a decrease in lift force. To compensate for this, the airplane needs to raise the angle of attack, which in turn will expose other parts at its underside [12].

There are four main types of icing which may occur on an airplane wing which effects the aerodynamics differently. These are: roughness, horn ice, streamwise ice and spanwise ridge. These are presented in Figure 4 where they are positioned based on their increasing aerodynamic effect and their two-dimensionality [5].

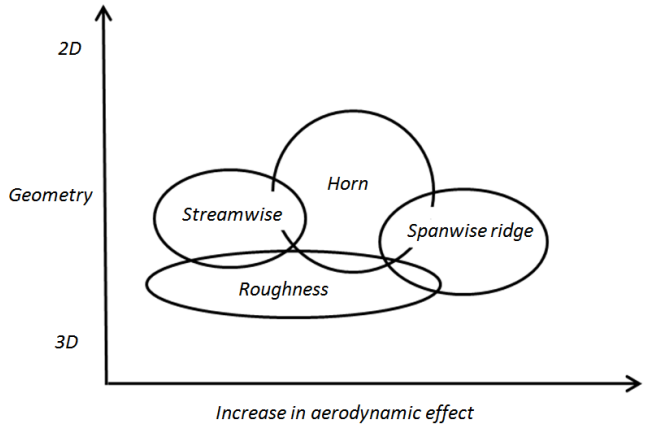

Figure 4 – Description of aerodynamic effects for different types of ice

Roughness ice is created at the early stages of ice accretion and takes no particular form. Its aerodynamic effect can vary greatly and it is largely 3D dependent. This means that the roughness ice can vary greatly along the width of the wing and local types of ice, such as a horn, may be created. The streamwise ice has a low aerodynamic effect and has no big gradients along the span of the wing. It is created when the droplet sizes are small and when it freezes quickly upon impact. It creates a layer on the tip of the wing which follows its curvature. The spanwise ridge ice is created when any kind of de-icing at the tip is used. The ice will then be gathered just outside of the de-icing zone of the wing, creating horn-shaped ice at both upper and lower surface. Because of their position, these can have a major effect on the aerodynamics. The last type of ice is the horn shaped ice which normally has one or two horns and it is generated when big droplets of water hits the wing which do not

solidify immediate upon impact. An example of a two-horned ice can be seen in Figure 5.

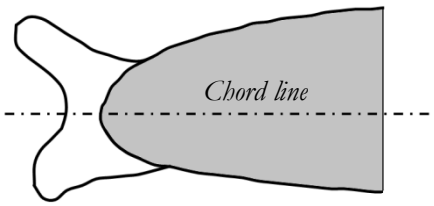

Figure 5 – Example of a two-horned ice shape

Horned ice may also include feather formations downstream of the horn, a feature which is not displayed in this figure. These horns will create local flow separations behind it, similar to the ones happening to a blank wing at high angle of attacks. Unless the angle of attack is great, the separated air will reattach to the wing surface at a point after the ice depending on the angle of attack, as displayed in Figure 6 [5].

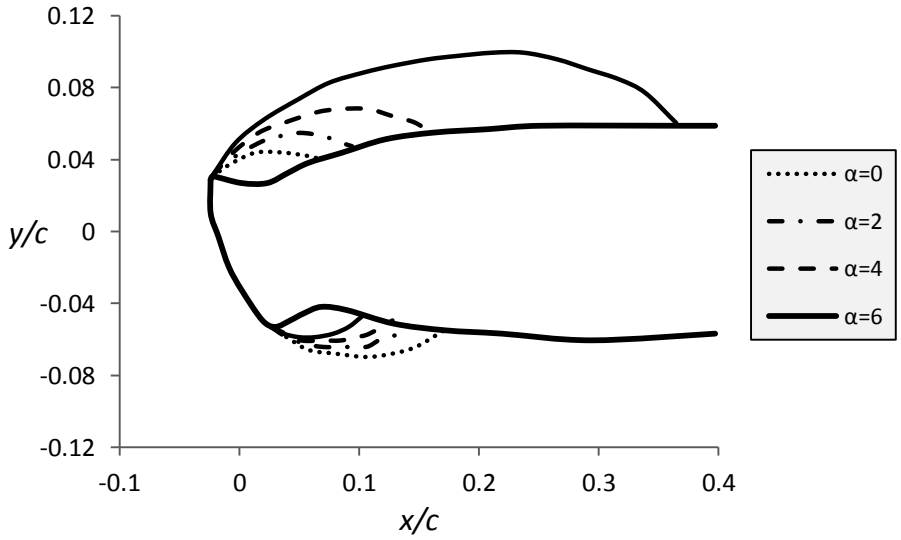

Figure 6 – Flow separation after horned ice at different angles of attack

These flow separation regions are characterized by turbulence and reversed and unsteady flows [5].

Even very small layers of ice will have noticeable effect of the aerodynamics, since ice effectively destroys the smooth flow of air on the wing. Previous tests have shown that an ice layer of equal thickness and roughness as a coarse sandpaper can reduce lift by 30 % and increase drag with up to 40 %. According to statistics between 1990 and 2000, 12 % of all weather associated airplane accidents are caused by icing [12].

3 Equipment and software description

For this thesis work, a number of different equipment and software have been used.

3.1 Wing replica

The wing replica, onto which the ice is mounted, has an airfoil which matches the shape of a cross section of an actual airplane wing but is scaled to a factor of 1:10. Its width (w) is 0.5052 m which includes two endplates, 3 mm each and the chord length (c) is 0.162 m. The shape of the airfoil is constant along the entire length. On the right end of the wing, a steel bar is placed which is used to mount it to the three component balance used for the wind tunnel. The wing is displayed in Figure 7.

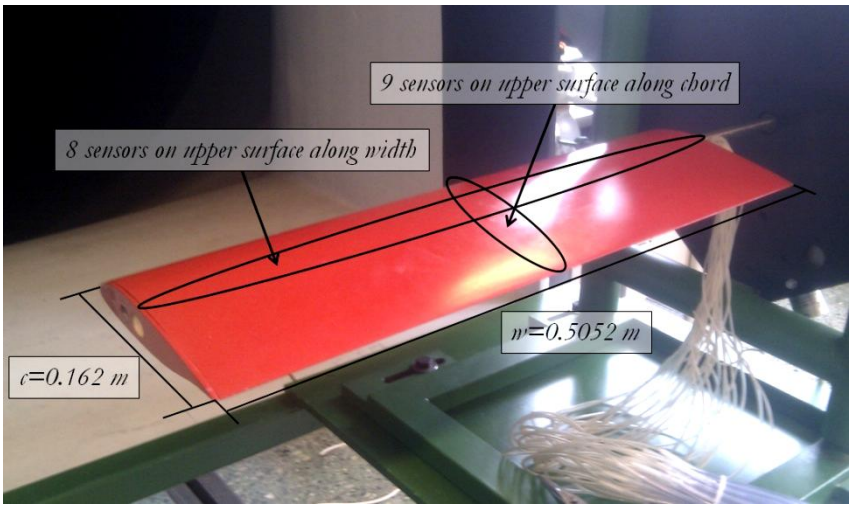

Figure 7 – The wing mounted to the three component balance

The wing is made out of wood and inside it are a number of strategically placed static pressure sensors. At the center of the wing, nine sensors are positioned at the upper surface from the leading to the trailing edge and nine at the lower surface (which are not seen in Figure 7). They are closer to each other at the front since the pressure gradients are higher there. There are also eight additional sensors positioned along the width which are used to calculate the pressure loss due to induced drag. Each pressure sensor has its own plastic tube running out from the wing and connects to a pressure balance board.

3.2 Rapid prototyping machine

To create the plastic parts from CAD files, a Rapid Prototyping Machine (RPM) is used since no other equipment capable of manufacture the required parts is available at the university. This machine is basically a printer which prints a model in three

dimensions by heating up a plastic material which builds up the model from bottom to top, layer by layer. The machine is unable to rotate its nozzle and is always pointing downwards, which makes it difficult to generate smooth diagonal surfaces.

In the software of the RPM, the user decides the position the part is to be printed in and how much support material to be used and the scaling. The support material is a weaker kind of plastic which is only deposited for stability during the creation process and is removed afterwards.

3.3 Wind tunnel

The wind tunnel has a cross section of 1x1 m and it is able to produce a wind velocity of up to 40 m/s. The velocity is set as a frequency and the wind velocity is measured using a velocity anemometer. To be able to use the wind tunnel for measurements, some other components need to be used together with it, which are described below.

The wing replica is fastened onto a three component balance, as can be seen in Figure 8.

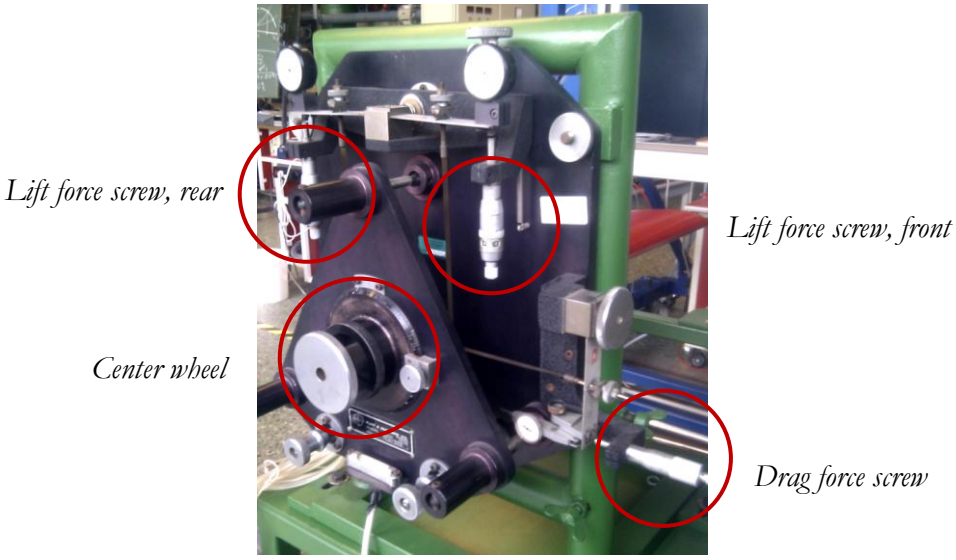

Figure 8 - The three component balance from Plint and Partners Ltd.

The angle of attack is adjusted using the center wheel and it is locked using a small clamp. The lift force may be determined using the two metal plates at the top that will be forced down as lift increases. The displacements of the plates are read using two micrometer screws, one for the front lift and one for the rear lift. The drag force is measured using the plate to the right of the three component balance which is also read using a micrometer screw.

The static pressure distribution over the wing can be read by connecting the pressure tubes from the wing replica to the pressure balance board which can be seen in Figure 9.

Figure 9 - The pressure balance board displaying the static pressure over the wing

The static pressure for each sensor on the pressure balance board is represented by a column of water. The tube to the right is the front-most sensor at the upper surface of the wing, the next is the front-most sensor at the bottom and so forth. A water level above the line indicates a negative static pressure and levels below indicates a positive static pressure. The result after measuring with a ruler is of the unit mmH_2O.

It is possible to measure the total pressure at the wake of the airfoil by using a pitot tube which is fastened to a traverse. The total pressure is read digitally by using an anemometer or by measuring the alcohol level on a manometer and then transferring it to Pascal. By moving the pitot tube up and down behind the wing it is possible to find out the total pressure loss which can be calculated into a drag force. How to calculate this is explained in chapter 4.6.3.

3.4 Engauge digitizer

Engauge digitizer is an open source software [1] which may be used to convert a graph into numbers. For example, if a graph is showing statistical data as a curve in a document but the raw data for the graph is missing, Engauge digitizer may be used to extract these. By importing the graph into Engauge digitizer, it is possible to extract the actual coordinates for the curve by following three steps: 1) the graph is discretized, meaning to filter the graph to only see the necessary curves. 2) Three points are placed on the x- and y-axis with defined values to set a coordinate system. 3) The curve is specified by using the software's automatic curve tracing where possible, and/or manually marking the curve. The end result is a list of coordinates for the curve using the specified coordinate system.

4 Methodology

The ice layer was constructed by extracting coordinates of a simulated ice shape with the software Engauge Digitizer, which were used to create a CAD file in Pro/Engineer. Once the CAD-model was created, a prototype was made in the RPM. This machine produces a plastic replica of the CAD model. The prototype was examined and the problem solving iteration process started. When the ice layer was completed, it was mounted onto the wing and tests on drag and lift forces were made in the wind tunnel. These results were compared to tests of a blank wing as well as results from simulations in Ansys Fluent.

An overview of the working process can be seen in Figure 10. It consists of seven main steps with corresponding sub steps.

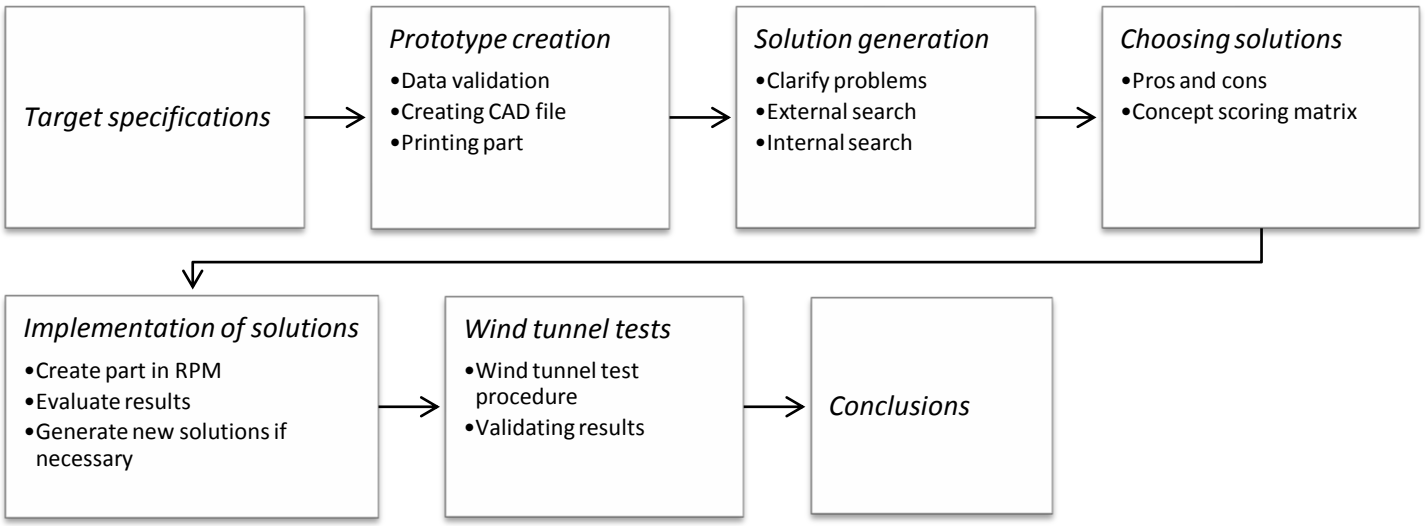

Figure 10 – Overview of the working process [13]

The five first parts of the process can be seen as a simplified product development process [13] with some modifications. The product being developed in this case is an ice layer and the customer is the wind tunnel tests. One can say that the product development process begins with the creation of the first prototype, since the main concept is more or less pre-determined. The following two steps, to generate and to choose the solutions, can be seen as steps in design for manufacturing, since the problem in this case is mainly how to produce the product in the best possible way and to ensure that it is good enough for its purpose, the wind tunnel tests.

4.1 Target specifications

The target specifications are set for the final ice layer as a way to guide the creation process [13]. Since there is no real customer, no identification of customer needs is made and thus the target specifications will be defined by the project itself. The specifications are not made as a list of metrics with different important factors and marginal and ideal values since all the specifications in reality are requirements that must be fulfilled by the finished ice layer.

4.2 Prototype creation

To find the best way to produce the final ice layer, an initial prototype needs to be made. This prototype can be considered as mainly made for learning purposes and to answer two questions [13]: "Will it work?" and "How well does it meet the target specifications?". The process of creating the prototype, evaluating it and generate and implement solutions should be repeated until these two questions can be positively answered.

The creation of the prototype is made in three steps: data validation, creating CAD file and printing the part. Data validation needs to be made in order to verify that the raw data of the ice layer is correct. A method then needs to be found for how to transfer the raw data into Pro/Engineer and to create a CAD model of these. The actual printing of the part should then only be a matter of loading the file into the 3D printer and print it.

4.3 Solution generation

The steps taken after a prototype is made may be seen as a concept generation process where a new concept needs to be found to fix the problems of the current prototype. The solution generation is made in two steps; clarification of problems, and internal/external search for solutions.

After a prototype is finished, it is examined and a list of problems is made. These problems are not assigned weight factors, since all problems are considered to be vital to solve. It is of great importance to find as many problems as possible early, to avoid the need for more prototype creations.

After the problems have been defined, solutions for them need to be found. The methods of finding these are by individual and group brainstorming and by consulting experts. Since this "product" is unique, the solutions to the problems could be hard to find externally. There are basically no lead users, patents, literature or benchmarking available that could help. The only external sources that can be used are experts in some areas. For example, the carpenters at the universities' workshop could be considered as experts for some of the occurring problems. The main method of finding the solutions has been individual brainstorming using related stimuli [13], such as the wing and the prototypes. The ideas were then discussed with the supervisors and further developed or combined with other solutions.

4.4 Choosing solutions

Two main tools have been used when deciding the best solution to problems: pros and cons lists and concept scoring matrices as described by Ulrich and Eppinger [13]. Each problem with more than one possible solution is presented with a pros and cons list. This list is made to force additional thinking and to come up with more positive and negative aspects of the solution that may not have been apparent from start. If the pros and cons list generates an apparent best solution, this goes through to implementation. If, on the other hand, the choice is still difficult, a concept scoring matrix is made.

A concept scoring matrix is first set-up by listing all the ideas as columns and then a number of selection criteria as rows. Selection criteria are features that the solution should have, for example durable and easy to mount. Each of them is set with a weighted percentage where a high value indicates an important criterion. Each solution is then given a rate of 1 to 5 for each selection criterion depending on how well the solution satisfies it. A total score for each solution may then be calculated using the following equation:

$$S_j = \sum_{i=1}^{n} r_{ij} w_i \quad [eq. 5]$$

Where:

r_{ij} = raw rating of concept *j* for the *i*th criterion

w_i = weighting for ith criterion
n = number of criteria
S_j = total score for concept j

The solution with the highest total score should be the best solution, but doesn´t have to be. If two or more concepts are still very even, it might be possible to combine two or more solutions and create a better one. The criteria and their weightings as well as the rating of the solutions are of course hard to set "right". When uncertainties have occurred, discussions with a supervisor have proved helpful.

A concept scoring matrix method is a good way of deciding the best solution since it forces one to carefully think through what the solution needs to fulfil and how important each feature really is. The method is time consuming though, and that is why the pros and cons list is made prior to the concept scoring matrix [13].

4.5 Implementation of solutions

The chosen solutions are implemented to the new part which is created in the RPM. If the results are satisfactory, the project proceeds to the wind tunnel tests. If not, a number of previous steps are repeated until an ice layer has been completed which fulfils all the requirements.

4.6 Wind tunnel tests

The wing is tested both with and without an applied ice layer. The purposes of the tests with the blank wing are twofold: The first is to make sure that the measurement methods are correct and that they give trustworthy results by comparisons to theory and Fluent Simulations. The other purpose is to attain data which can be compared to tests with the iced wing.

To measure the aerodynamic effects on an airfoil in a wind tunnel, the wind tunnel needs to be set up properly, the raw data needs to be extracted and the results needs to be processed.

4.6.1 Preparations

The wind tunnel is turned on and its frequency is raised so that the air velocity is approximately 22 m/s. The velocity is controlled using a velocity anemometer. The velocity of the wind should, in theory, not affect the outcome of the tests since the output values, C_L and C_D, are dimensionless. But if the velocity is too low, the forces will be hard to measure correctly and if the velocity is too high the wing might start to wobble too much to assure accurate readings.

The wing is attached to the three component balance using its steel bar on its right side. The wing is adjusted to an angle of attack of 0° using a water leveller.

Once the preparations have been made, the data acquisition begins. What can be measured is the lift and drag forces on the wing for varying angles of attack.

4.6.2 Measuring the lift force

There are two ways of measuring the lift force. Both methods should give the same end result and by comparing them one can get a sense on how reliable the results are. If they are similar, the probability is high that the result is accurate. If they on the other hand are not similar, one (or both) method should be faulty and it will have to be elucidated before proceeding.

Method 1 - Force

The first method is to directly measure the lift force using the three component balance as explained in chapter 3.3.

Before the wind tunnel is started, the values on the two lift force micrometer screws are read and the difference between the starting value and the following values with the wind tunnel turned on is the change in lift force. The delta value for the front reading is then multiplied by the spring constant, *C*, for the front spring and vice versa. The sum of the front and rear values is the lift force of the wing for the current angle of attack.

$$F_L = F_{L\,front} + F_{L\,rear} \; [eq.6]$$

Where:

$$F_{L\,front} = C_{front} \times \Delta F_{front}$$

$$F_{L\,rear} = C_{rear} \times \Delta F_{rear}$$

Note that the actual lift force is dependent on the wind velocity, the physical size of the wing and the density of the air. The lift force is therefore an unsuitable parameter for comparisons. To calculate the dimensionless lift coefficient the following equation is used:

$$C_L = \frac{F_L}{\frac{\rho}{2} v^2 cw} \; [eq.7]$$

Note that equation 7 can be derived from equation 3.

Method 2 - Pressure

The second method uses the pressure distribution board as explained in chapter 3.3.

The measured mmH_2O values from the pressure distribution board are transferred to Pascal by multiplying it with 9.8066. Pascal is of unit N/m^2 and to transfer the Pascal values into a force it needs to be multiplied by an area. The width, w, is 0.5052 m for all pressure sensors but the length varies depending on its position.

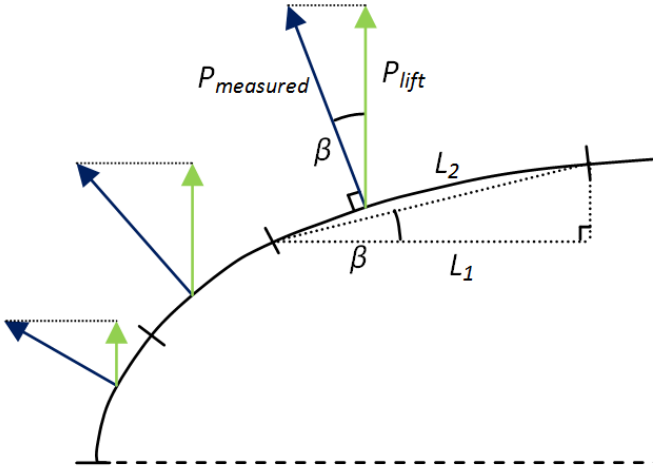

Figure 11 - Blue arrows represent measured pressure from sensors and green arrows is the portion of it contributing to the lift force

The length that corresponds to each sensor can be seen in Figure 11. The markings on the airfoil between the pressure vectors divide the surfaces into different sized lengths where the pressure acts. Two simplifications are needed; 1) the measured pressure is seen as the average value for its area and; 2) the pressure length does not take the curvature of the airfoil in regard and uses the linear length, L_2, instead. The sensors on the wing have been positioned in such a way that this simplification should have a total effect on the results of less than 5% [14].

The length, L_2 for sensor x, in regard to the angle β and horizontal length L_1 is equal to:

$$L_{2,x} = \frac{L_{1,x}}{\cos(\beta_x)} \quad [eq.8]$$

The pressure that is measured is not the one directly linked to the lift force. As can be seen in Figure 11, the measured value, $P_{measured}$, is normal to the surface of the wing, but the pressure that contributes to the lift is the pressure vector normal to the chord of the wing, P_{lift}. The lift pressure, P_{lift}, in Pascal for a sensor x in regard to angle β and measured pressure is equal to:

$$P_{lift,x} = P_{measured,x} \times \cos(\beta_x)\ [eq.9]$$

The actual local lift force for one sensor x in Newton becomes:

$$F_x = P_{lift,x} \times 9.8066 \times L_{2,x} \times w\ [eq.10]$$

By inserting equation 8 and equation 9 into equation 10 we get:

$$F_x = P_{measured,x} \times \cancel{\cos(\beta_x)} \times 9.8066 \times \frac{L_1}{\cancel{\cos(\beta_x)}} \times w\ [eq.11]$$

$Cos(\beta_x)$ cancels out and we get an equation for the lift force for one sensor without regard to the angle:

$$F_x = P_{measured,x} \times 9.8066 \times L_{1,x} \times w\ [eq.12]$$

The total lift force for a wing of infinite length is the integral of the pressure distribution on the wing. This is calculated by summing up the forces for all sensors on the lower surface and subtracting this with the sum of all sensor forces on the upper surface. Since F_x is perpendicular to the chord, the actual lift force also needs to take the angle of attack into account by multiplying the force with cosine α:

$$F_{L,infinte} = \left(\sum_{i=1}^{x} F_{x,lower\ surface} - \sum_{i=1}^{x} F_{x,upper\ surface}\right)\cos(\alpha)\ [eq.13]$$

This equation is the area of the static pressure distribution over the airfoil. Figure 12 shows an example of how such a distribution could look like [10].

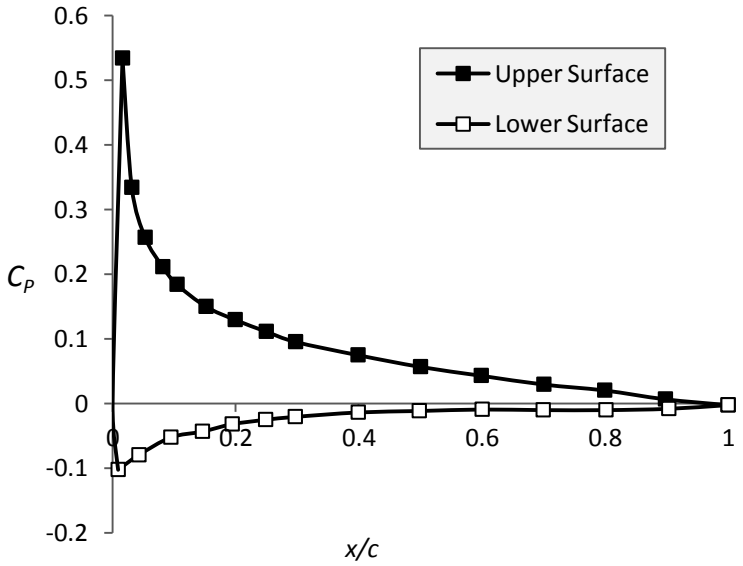

Figure 12 – The static pressure distribution of a NACA 0012 airfoil, α=9°

Note that the y-axis is inverted so that values from the upper surface (with a lower pressure than the free stream) are the top curve. By studying equation 13, we see that the lift force becomes negative if the upper surface has a positive pressure and the lower has a negative pressure, which is the case for most negative angles of attack. This is the lift force for a wing of infinite length, since it assumes no lift losses due to induced drag. To get the lift for a finite wing, the induced drag needs to be taken into account.

Figure 13 shows how the pressure could be distributed along the width of a wing [10].

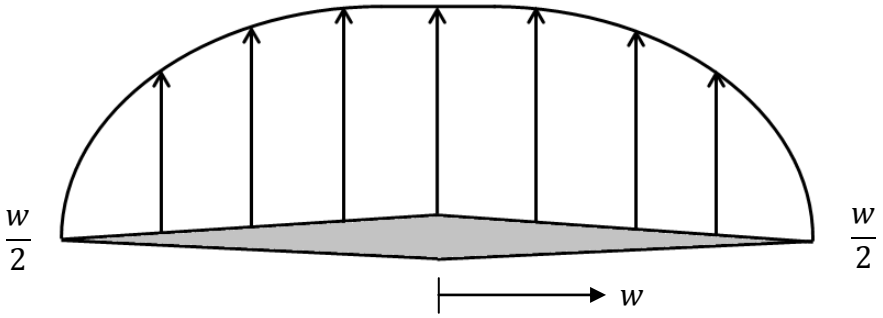

Figure 13 – Example of pressure distribution along wing width, front view

The pressure distribution along the width of an infinite wing would have the maximum pressure all the way to the ends, but this is not true for a finite wing. The lift force for a finite wing with the induced drag taken into account is calculated by dividing the pressure area of a finite wing (such as the one in Figure 13) with the pressure area for an infinite wing, which is described as the pressure at the centre of wing multiplied by the wing width. The lift loss is described in equation 14.

$$Lift\ loss = 1 - \frac{Pressure\ area\ of\ finite\ wing}{Pressure\ area\ of\ infinite\ wing}\ [eq.14]$$

The lift loss is dependent on the length of the wing. A long wing does not suffer as much loss in lift as a shorter one. The total lift force across the entire wing is thus:

$$F_{L,finite} = F_{L,infinite} \times Lift\ loss\ [eq.15]$$

The lift coefficient, C_L, is then calculated using equation 7.

4.6.3 Measuring the drag force

The two methods of measuring the drag force are similar to those of measuring the lift force. The first method uses the instrument on the three component balance and the second measures the pressure in the wake behind the wing using a pitot tube.

Method 1 - Force

The first method is to directly measure the drag force using the three component balance as explained in chapter 3.3.

Before the wind tunnel is started, the value on the drag force micrometer is read and the difference between the starting value and the following values with the wind tunnel turned on is the change in force. This value is multiplied by the spring constant to get the drag force for each angle of attack.

$$F_D = C \times \Delta F \ [eq.16]$$

To calculate the dimensionless drag coefficient, the same equation as for the lift coefficient is used:

$$C_D = \frac{F_D}{\frac{\rho}{2} v^2 cw} \ [eq.17]$$

Method 2 - Pressure

The second method uses the pitot tube to measure total pressure at the wake of the airfoil as explained in chapter 3.3.

The procedure of measuring the total pressure starts by placing the pitot tube as close to the trailing edge as possible at the middle of the wing. This value is set as the reference point for the traverse. The pitot tube is then moved up and down behind the wing in different intervals depending on the angle of attack (with a minimum of 1 mm) and the total pressure is read for each position. When using the manometer, the values are translated from mmAlc to total pressure with the following equation:

$$P_{tot} = \frac{mmAlc \times 0.8 \times 9.8066}{2} \ [eq.18]$$

When using the anemometer, the Pascal value is read directly on the display.

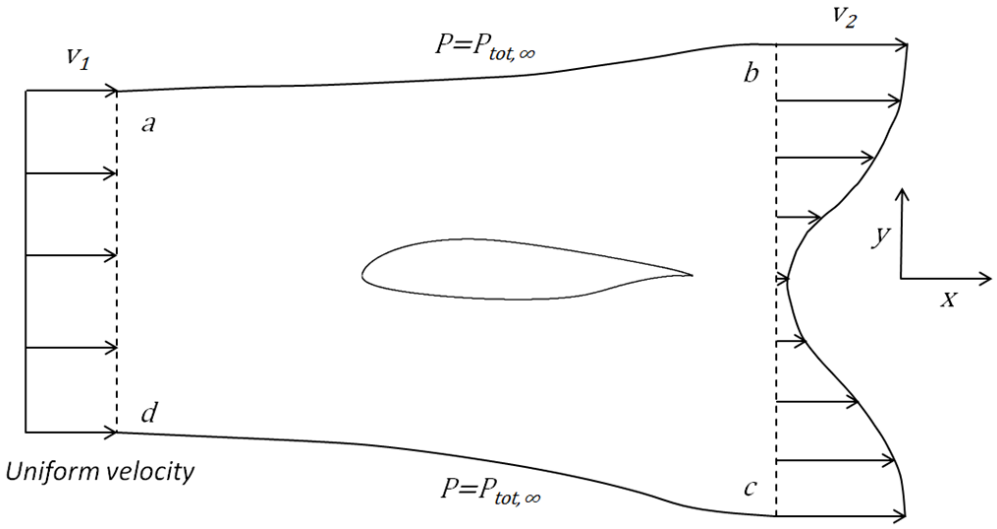

Figure 14 – Velocity profiles ahead of and behind of an airfoil

Figure 14 shows the velocity profiles around an airfoil [10]. The incoming air velocity is uniform ahead of the airfoil (*a-d*), but as the airfoil splits the air, the velocity profile changes. If the velocity profile at the wake of the airfoil has been measured and constant density is assumed, the drag force per unit width may be calculated using the following equation [10]:

$$F_D = \rho \int_c^b v_2(v_y - v_2)dy \; [eq.19]$$

In this case, the pitot tube measures the total pressure and not the velocity. Since $P\ [kg/ms^2] = \rho\ [kg/m^3] \times v^2\ [m^2/s^2]$, equation 19 may be rewritten as:

$$F_D = \int_c^b \left(P_{tot,\infty} - P_{tot,y}\right)dy \times w \; [eq.20]$$

The width, *w*, is added to include the width of the wing since equation 19 is per unit width. The drag coefficient is then calculated using equation 17.

4.7 Ansys Fluent

In addition to comparing the wind tunnel results from the blank wing to the iced wing, a simulation of the blank wing is made in Ansys Fluent.

A 2D model of the correct airfoil had previously been made and was used for these simulations. Note that as the airfoil is in 2D, it has no length and is thus considered to be an infinite wing with no lift loss due to induced drag. To get the results for a finite wing, the calculated lift losses using the wind tunnel for the blank wing will be used

for the Fluent methods. This way, they are easier to compare to the wind tunnel results. As the Fluent model is in 2D, it will not be possible to compare the lift loss due to induced drag with the wind tunnel tests.

One adjustment to the model was made by adding an enhanced wall treatment which is able to better capture the gradients close the surfaces as well as the separation of flows. It´s possible to use it because the mesh is fine enough in the near wall region to be able to resolve the laminar sublayer which defines the border between laminar and turbulent flows [15].

By changing the direction of the incoming air, it was possible to simulate any angle of attack. The wind velocity, air density and airfoil size are all set to equal values as the wind tunnel experiments. In Fluent, there are also two ways of extracting the drag force and two ways of extracting the lift force. The easiest method is to use the automatic function which calculates the lift and drag coefficients based on set reference values, such as chord length and wing width. The other way is to use the same method as the pressure methods described in chapter 4.6. The static pressure on the upper and lower surface of the airfoil can be extracted by writing a coordinate file of the wing position x and the corresponding pressure. The total pressure at the wake of the airfoil is also written to a coordinate file by creating a line at the trailing edge with an angle perpendicular to the incoming air. These values can then be used in the exact same manner as previously described.

It is then possible to compare these results with the wind tunnel results and conclude if they match or not. If they match, this gives a clear indication that the results are trustworthy. Another way of verifying the results from the wind tunnel tests is by comparing it to previously made studies. Since all airfoils have different lift and drag coefficient curves, it is hard to compare the wind tunnel results with any previously made study unless it is the exact same airfoil, which is hard to know. What one can compare, though, is the shapes of the curves and the effect of a similar horn-shaped ice layer. One can, for example, see how much the stall angle is lowered and how the shapes of the curves relate to each other.

5 Ice layer development process

This chapter present the results from the ice layer generation process.

5.1 Ice layer specifications

A finished ice layer must fulfil the following criteria:

- The shape of the ice layer shall correspond to the simulated shape
- The shape is constant along the width
- The ice layer does not fall off during wind tunnel tests
- It´s easy to remove the ice layer after tests without any damages to the wing
- The ice layer does not block any pressure sensors on the wing
- It should be possible to ensure that the ice is positioned correctly on the wing

All of these are considered to be of the same importance and they specify the necessary requirements of the ice layer.

5.2 The first prototype

The purpose of the first prototype was not to create an ice layer ready for mounting on the wing, but rather as a help in finding problems which needs to be solved before the creation of the actual ice layer. To make the first prototype, three steps were taken; data validation, creating CAD model and printing of the part.

5.2.1 Data validation

The shape of the first ice layer is taken from a previous study from an internal document at the University of Applied Sciences [14]. In this study, ice shapes on different locations of a wing has been simulated using NASA's Lewis Ice Accretion Prediction Code (LEWICE 1.6) [3]. The generated ice shape that corresponds to the same airfoil as the existing wing replica can be seen in Figure 15. The position of the ice on the wing is the root of the wing, closest to the body of the airplane.

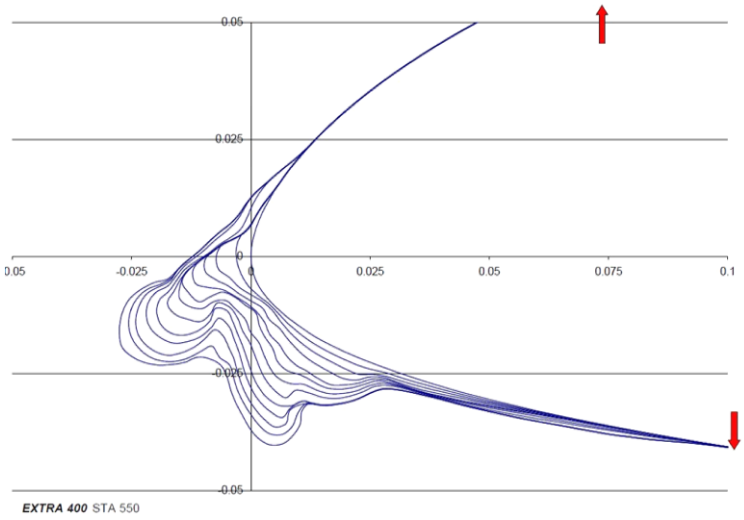

Figure 15 – The shape of the ice layer as simulated by the LEWICE code [14]

The input for this simulation was a flight height of 2400 m (8000 feet), a calibrated air velocity of 66.7 m/s (130 KCAS), a temperature of -5°C, a rain droplet size of 25 micrometer and a cloud liquid water content (LWC) of 0.5 g/m^3. The different curves of the ice in Figure 15 symbolize the different time steps in the simulation where the outer curvature is the shape after a 45 minutes flight.

As can be seen, this is an ice layer of a horn type. One can argue that it got one or two horns but as both horns affect the lower surface, it is considered a one horned ice. A horned-shaped ice is fitting for a number of reasons. It has low 3D dependence (small variations along the width) as can be seen in Figure 4. This means that the simplification of no gradients along the width of the wing has a small effect on the results. Figure 4 also shows that a horned shaped ice has a high effect on the aerodynamic performance, which makes it easier to compare the results and to draw conclusions. Compared to the other types, a horned-shaped ice will be easier to create for two reasons. The first is that it´s thicker than the outer types which make it easier for the RPM to generate an accurate profile. The second reason is that it won´t be necessary to make a correct roughness to the surface of the ice. According to M.B. Bragg *et al.* [5]: "Roughness does not seem to play a major role in the aerodynamics of airfoils with horn ice shapes". So the roughness can be neglected without a major effect on the results.

In order to use this ice shape, it had to be validated that the study uses the same coordinates for the airfoil as the airfoil of the wing replica at the university. This was made by using the software Engauge Digitizer to transfer the graph of the airfoil in Figure 15 into coordinates. These were inserted into an Excel-file together with the

coordinates for the actual wing. The comparison between the two is shown in Figure 16.

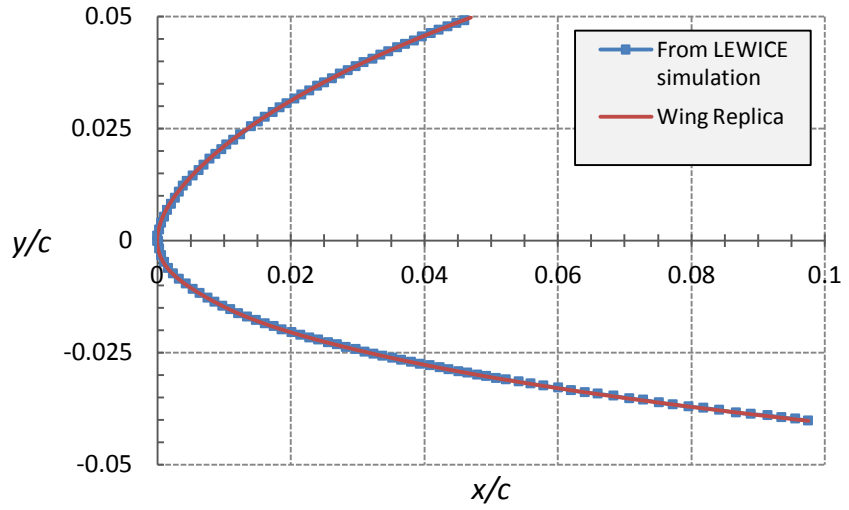

Figure 16 – Airfoil shape comparison of wing replica and LEWICE simulation

By studying the graph, it is evident that the airfoil used in the ice simulation has the same shape as the wing replica.

5.2.2 Creating CAD model

The creation of the CAD model required two steps to be taken: 1) Using Engauge Digitizer to find out the coordinates for the ice layer shape and 2) import these into the CAD software Pro/Engineer. Once imported, the coordinates are used to create splines to use for extrusion.

To find out the coordinates for the ice layer, the same procedure as with the airfoil shape was applied. The method of transferring a list of coordinates into a solid part in Pro/Engineer is not obvious. The method that was eventually found was to transfer the coordinates from Engauge Digitizer into a ".pts" file with three columns; x-, y- and z-value (z-value is 0 for all coordinates). This file could then be used in Pro/Engineer by creating a new coordinate system for reference and a 2-point spline. By opening the spline, it was then possible to import the coordinates from the external coordinate file, so that the spline got the shape defined by the coordinates.

The ice layer could be created by first extruding the ice layer spline and then removing the necessary material from it by extruding the airfoil shape.

5.2.3 Printing the prototype

The CAD file of the prototype created in Pro/Engineer was converted into an .stl file format which is commonly used for rapid prototyping since it saves only the surface geometry of the model. The .stl file was then imported to the software of the RPM and the model was printed in a vertical position to assure best accuracy, since the nozzle of the RPM is always pointed downwards. Figure 17 shows the finished part.

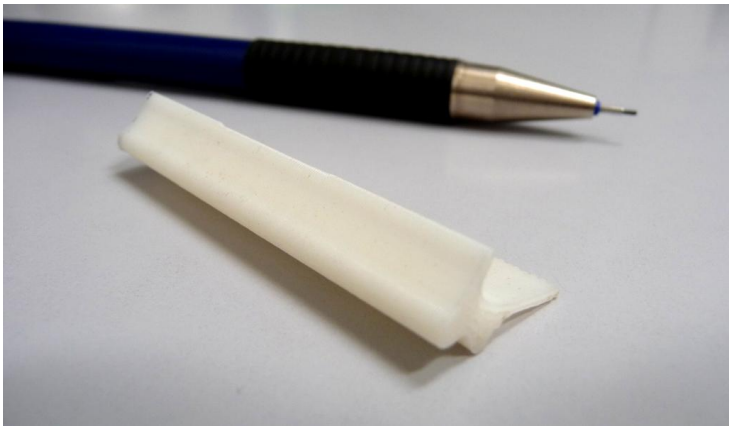

Figure 17- The finished ice layer in size comparison to pencil. Length: 50 mm

The finished part felt durable, even on the thinnest part, and will most certainly not break during wind tunnel tests. The layers can be seen and felt but are small and should not have an impact on the result. The profile at the tip of the ice looks just as the computer model and is satisfactory.

5.3 Clarifying problems

The purpose of the first prototype was to find problems that may occur. The identified problems that needed solutions were:

a) **Fitting the ice.** The ice did not fit to the wing. Either the ice shape or the shape of the wing tip (or both) is faulty. See Figure 18.

b) **Positioning the ice.** The ice layer needs to be positioned at the exact correct location to ensure good wind tunnel results. It is also important that the ice is positioned correctly along the width of the wing.

c) **Making the thinnest parts.** The thinnest parts of the ice layer should be as thin as possible. The rapid prototyping machine proved only to be able to create layers of a minimum thickness of around 1 mm.

d) **Attaching ice to wing.** The wing must not be damaged in any way by the ice layer. A method of attaching it to the wing without damaging it needs to be found.

e) **Pressure sensors.** The wing has a number of pressure sensors used to read pressure. These must still be usable.

f) **Maximum height.** The rapid prototyping machine can only create parts of maximum height 300 mm and the ice layer need to be 506 mm.

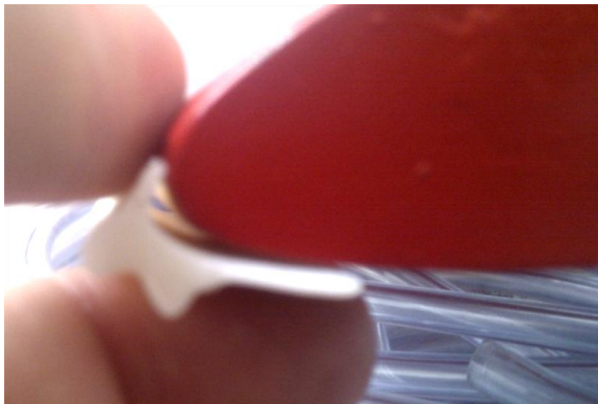

Figure 18 – The ice layer clearly does not fit on the wing tip

5.4 Solutions

In this chapter, a proposed solution for each problem in the previous section is presented and described.

a) Fitting the ice

The first hypothesis to why the ice didn´t fit was that the thinnest parts of the ice layer which were too thick changed the inner shape of the ice. A new ice layer was therefore made without these thin parts but it still did not fit. The conclusion was then that the wing shape must be faulty and to try this, two negative shapes were made as can be seen in Figure 19.

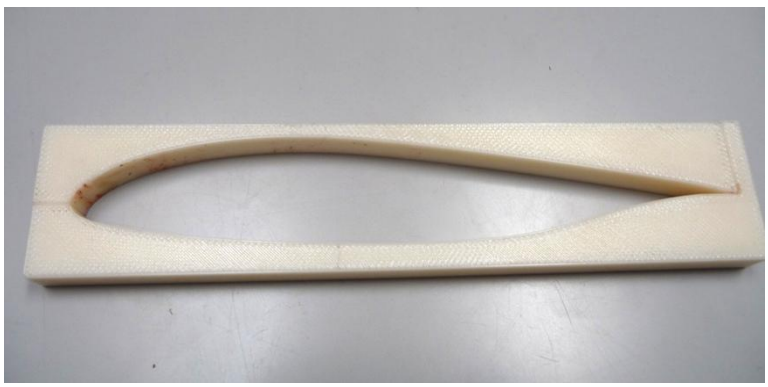

Figure 19 – Top and bottom negative forms for controlling shape of wing

These showed that the wing was too thick since it was impossible to put the tip parts of the negative forms together. It was still hard to decide exactly where the wing needed adjustments using the forms. Other methods to decide that had to be considered. By placing the wing upright on a paper and then using a pencil to draw its profile, it was possible to take a picture of the paper and then use Engauge Digitizer to find out the coordinates.

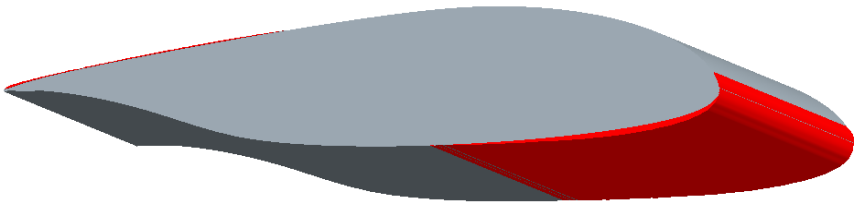

Figure 20 – CAD file with desired shape in grey and excess material in red

As can be seen in Figure 20, the front lower surface needs to be adjusted. The maximum thickness of the surface to be removed is 1.2 mm. This also seemed reasonable, based on what you could tell by using the negative forms. The other part that was also slightly inaccurate at the upper rear surface was considered to be of minor importance because of its position and small thickness. The wing was taken to the carpenter who was able to grind down the lower surface until the desired shape was achieved. This surface was then made smooth to ensure unbiased results.

b) Positioning the ice

At first, a pros and cons list was made where five possible solutions were evaluated as can be seen in Appendix A. The most promising solution from this list was to add an "end profile" plate which follows the curvature of the wing at the end of the ice layer. If this plate is positioned correctly to the wing, the ice should also be correct. A concept scoring matrix (in Appendix) was also made for this problem, since the pros and cons list didn´t give a definite answer. Here, the end profile and the negative form got the highest score and after some discussion it was decided to combine the two solutions. By also using a negative form, it was possible to improve another shortcoming of the end profile solution, good precision along the width of the wing.

Figure 21 – Negative form used to ensure a proper fit of the ice

Figure 19 shows the negative form of the upper surface, which was created to ensure a good fit along the width of the wing. Note that the shape of the top part of the ice is included at the tip.

c) Making the thinnest parts

Four possible solutions were found for this problem; plastelin, putty, grinding and ignore. The solution that came out on top using this pros and cons list (see Appendix) was to use a material called plastelin. The parts where the ice is thinner than 1 mm are simply not created in the rapid prototyping model and these gaps are instead filled with plastelin. One can compare plastelin to stearic acid (candle-wax) which comes as pellets, which first need to be heated up before they can be poured onto the desired location. After it has been solidified, it is easy to scrape off excess material until the desired shape is achieved. This should be durable, easy to remove without damage and with the possibility to create very thin layers. The cons with this solution are that it is time consuming and difficult to apply. To ensure that the shape is correct, the negative form used for positioning the ice, was used. By sliding it back and forth after applying the plastelin, it was possible to shave off the excess material and create a smooth surface along the width of the wing.

d) Attaching ice to wing

The first idea on how to attach the ice to the wing without damaging it was to use a so-called "post-it" glue, which is also used for post-it notes. One spray can was ordered and was tested with a previously made prototype. The result was disastrous since the glue made the paint dissolve. The most important part, the wing tip, sustained the least amount of damage, since most glue was placed on the end profile. The other solution to this problem was to use a sort of glue called "rubber cement" which was available at the university. It´s an adhesive made from elastic polymers which form a strong yet flexible bond which is easy to remove and doesn´t cause any

damage on wood. Testing proved that it had the desired effect and was thus chosen as the method of attaching the ice to the wing.

Problems e) and f) in the list on the previous section are easy to solve and did not require any special method. The ice never covered the pressure holes, so no solution for this was needed. The solution for problem f) was solved by dividing the ice into four separate parts. To ensure that these got connected properly, a male-female connection type was made on the ice where one side had a circular extension of a couple of millimetres while the other side got a circular hole in which to fit the other part.

5.5 Implementing solutions

After adjustments to the wing surface, the ice model fit satisfactory to the wing. The attachment of the four parts went smoothly using the rubber cement.

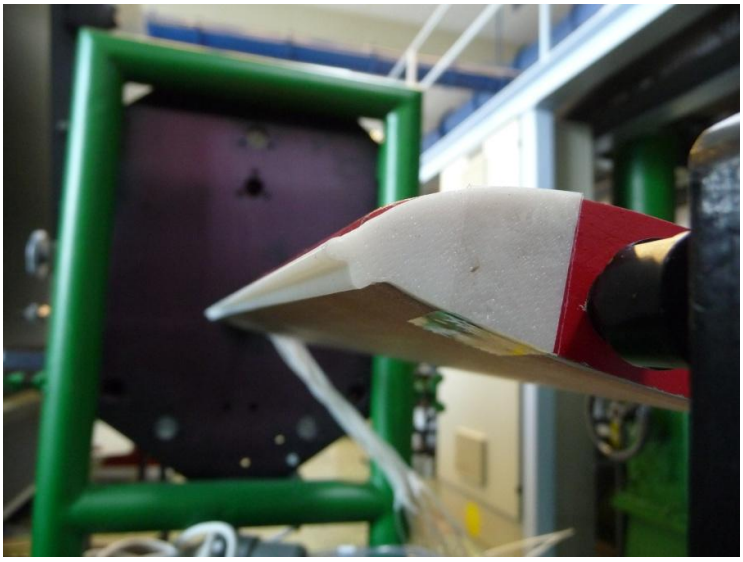

Figure 22 – The ice positioned on the wing

As can be seen in Figure 22, the end profile helped greatly in assuring a good position at the ends and the negative form was helpful in sideways adjustments. An extra tape was applied to the ends to make sure the ice layer did not move during solidification of the rubber cement. The joints between the four parts were very small and barely visible and should not affect the results. Also note in the figure that there is no paint on the lower surface which is due to the adjustments made by the carpenter. The shape as can be seen in Figure 22 is referred to as "ice 1" in the rest of the report. The second type of ice which is to be tested is referred to as "ice 2". Ice 2 includes a plastelin filling on the upper surface which represents the thinnest part of the ice layer which the rapid prototyping machine was unable to make. This division was made to

test the impact of the small plastelin layer. It was only put on the upper surface and not the lower for two reasons; 1) the lower surface has less impact on the lift compared to the bottom and 2) applying plastelin to the lower surface would cause two problems, it would block the pressure holes and it would require the creation of another negative form. If the difference between these two types of ice would prove to be minor, one could argue that the effect of the bottom plastelin is negligible. The process of applying the plastelin to the upper surface went easier than expected. It was done by first heating up the plastelin, then pouring it into the gap, letting it solidify and then using the negative form to shave off excess material. This was repeated three times until the desired result was achieved. The surface was smooth with small gradients along the width. It also became thin enough, since the transition between wing and plastelin could almost not be felt.

6 Wind tunnel test results and discussion

First, the blank wing was tested in the wind tunnel using both methods for lift and drag respectively. These results are then verified by comparison to the results from the Fluent simulations before continuing with comparisons with the iced wings.

6.1 Lift force

Figure 23 shows the static pressure coefficient distribution on the upper and lower half of the blank wing for different angles of attack. Values with white marker fills are values from the lower surface of the wing and those with solid fill are from the upper surface. These values have been measured using the pressure balance board which have been transferred from mmH_2O to pressure coefficients. The x-axis is non-dimensionalized by dividing the actual chord position x with the full chord length c to get the relative position on the wing.

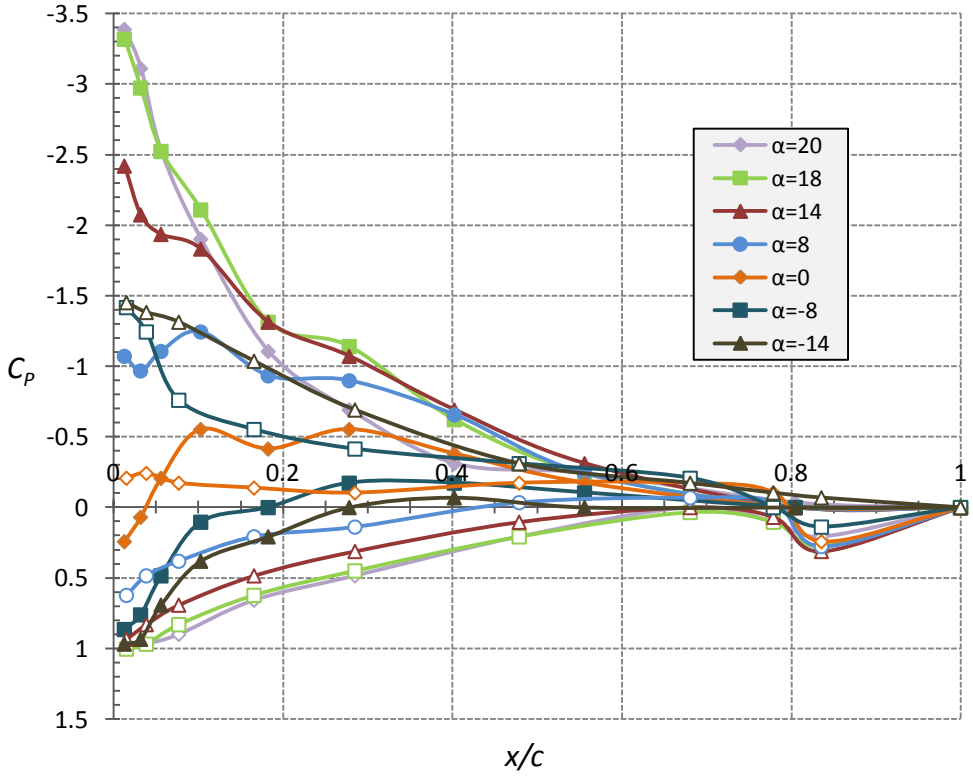

Figure 23 – Upper and lower pressure distribution on blank wing

A negative pressure coefficient on the upper surface and a positive on the lower surface help the lift force, while the opposite have a negative effect on the lift force. Both upper and lower curves seem to raise and fall in pressure respectively with an even interval up until an angle of attack of 20°, where the top curve drastically falls

and reducing lift. Note that the pressure at x/c=1 is always 0, which is an assumption since there is no sensor at this position.

By calculating the area defined by the static pressure distribution and making adjustment for the angle of attack, one can calculate the lift force for an infinite wing using equation 13. To calculate the lift force for a finite wing, the loss caused by induced drag needs to be taken into account as well.

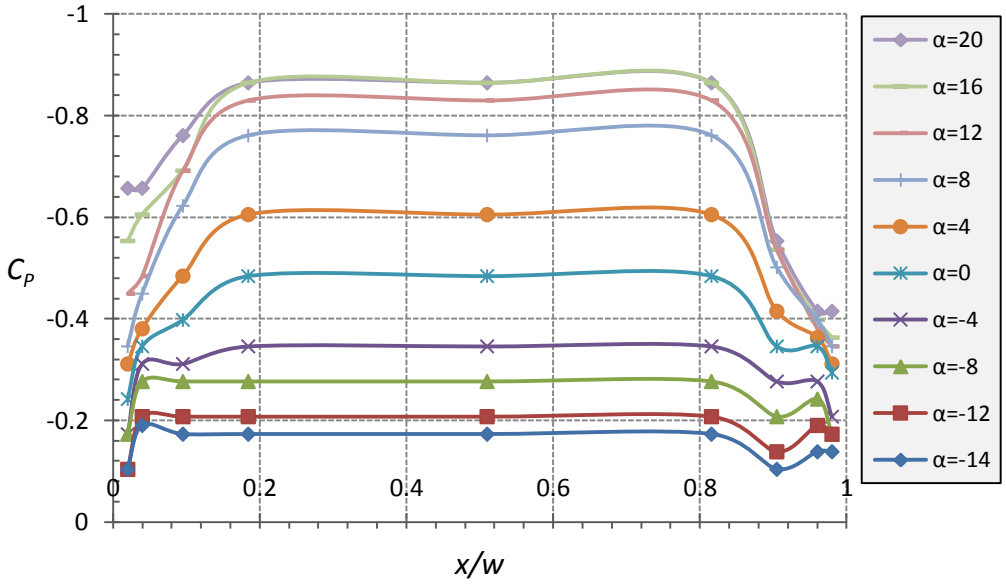

Figure 24 – The pressure distribution along the width of the upper blank wing for different α

Figure 24 shows the static pressure distributed along the width of the upper surface on the blank wing for different angles of attack. In this Figure, one can more clearly see that as the angle of attack is increased, the pressure coefficient gets lower due to a faster flow of air across the upper surface of the wing (the Bernoulli effect). Note that the three middle values are always equal. For the 4th sensor from the left, the plastic hose leading to the pressure distribution board was missing and could thus not be used. Because of symmetry, it was assumed that the pressure on this position is similar as the pressure at the 6th sensor, which was functioning. The center sensor is supposed to be the same as one along the chord and is supposed to be aligned with the ones along the width. This was not the case for this wing, and no center pressure sensor was thus available for use. Therefore, the center value is also set as equal to the 6th sensor from the left.

The pressure coefficients seem to be slightly higher on the right side of the wing, especially at higher angles of attack. This could be explained by the fact that the wing is not positioned in a symmetric fashion in regard to the wind tunnel; the right side

($x/w=1$) of the wing is closer to the edge of the wind tunnel compared to the left side. This could cause a lower wind velocity in this region, resulting in a higher pressure.

The lift losses caused by the induced drag at the ends of the wing for each angle of attack are presented in Table 1.

Table 1 – Lift losses in percentage caused by induced drag

α (°)	-14	-12	-8	-4	0	4	8	12	16	20
Lift loss, %	6.44	6.02	5.74	7.06	9.25	10.52	11.25	11.41	11.19	9.81

For all positive angles of attacks, the lift losses are about 10 %. The negative angles of attack, -14, -12 and -8 are also close to each other but with a value of around 6 %. This is hard to explain but should be an effect of the asymmetric shape of the airfoil. It is assumed that the same loss in lift occurs on the lower surface of the wing. These values were also measured for the iced wings and showed almost identical values.

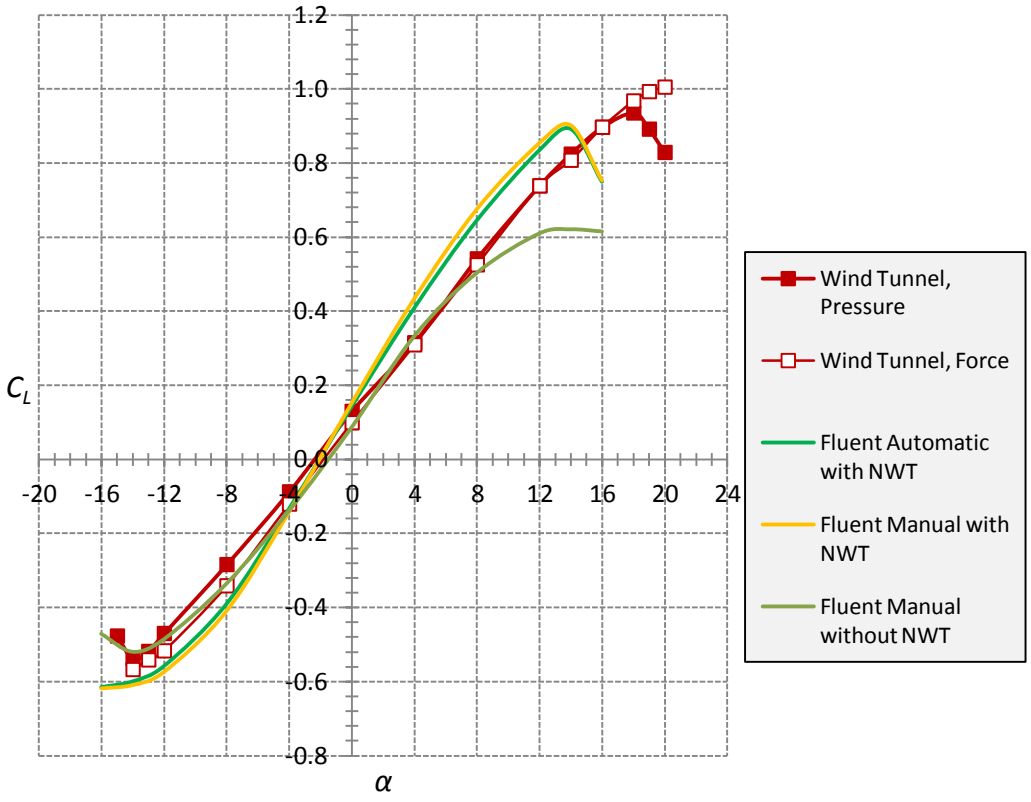

Figure 25 – Lift coefficient to angle of attack graph comparing wind tunnel results with Fluent results for a blank wing. NWT=Near Wall Treatment

By first comparing the direct force method and the pressure method from the wind tunnel test in Figure 25, one can see that they are more or less a perfect match for all

positive angles of attack up to 18°, where the wing starts stalling according to the pressure method. For angles of attack above that, the direct force continues to rise where the pressure falls. My hypothesis for this behaviour is that high angles of attack are hard to measure with the direct force measurement due to high drag forces on the wing which causes it to lurch up and down. The pressure sensors do not sense this wing motion and is thus unaffected. The pressure method in this graph has been adjusted with regard to the angle of attack and the induced drag to acquire the results for a finite wing. The direct force method measures this effect directly and no adjustment needs to be done.

Note that the wing actually has a lift force on an angle of attack of 0°, which is the case for asymmetric airfoils. According to Anderson [10], the lift force is typically zero at around -2° to -3° for an asymmetric wing. In Figure 25, the curves cross the x-axis at around -2°, which matches the theory.

By comparing the Fluent automatic method with the Fluent manual method using the near wall treatment (NWT) (see chapter 4.7), one can see almost no differences between them at all. This indicates that the manual Fluent calculations have been made correctly, and therefore also support that the pressure calculations based on the wind tunnel results should be correct, since the same method is used.

By comparing the manual Fluent result without the near wall treatment with the wind tunnel results, there is a close match for all angles of attack up 8°, where Fluent starts to stall while the wind tunnel results continue linear. It seems unlikely that the Fluent method without the near wall treatment should be a better solution and the hypothesis for this is that the match is a coincidence. Maybe the even surface without roughness in Fluent cancels out the less accurate calculation in the near wall region.

The comparison between the Fluent results using the near wall treatment with the wind tunnel results is much less of a match. The Fluent curves cross the wind tunnel curves at an angle of attack of -2°, at the exact point where the lift force is zero, but for all other angles, the Fluent methods are approximately 30% too high. The stall angle is also much earlier, at α=14° instead of at α=18° for the pressure method for the wind tunnel. The reasons for these differences are hard to explain. The 30% deviation could be explained by the fact that Fluent does not use any surface roughness, which improves the lift force. The shape of the wing replica is also not identical to the one used in Fluent. The wing replica does have some minor uneven surface areas. The early stall angle could be because Fluent still is unable to capture the complex separation of flows in a correct way. Of course, it could also be that the

wind tunnel results are inaccurate, though this seems more unlikely, since both independent wind tunnel measurements are similar up to α=18°.

Unfortunately, these results do not give a convincing answer as to whether or not the results from the wind tunnel are reliable. The hypothesis is that the pressure method is still showing correct values since it agrees with the direct force method and it shows a stall angle. The Fluent simulations could also be correct but the shape and surface of the model is too different from the actual wing to compare them.

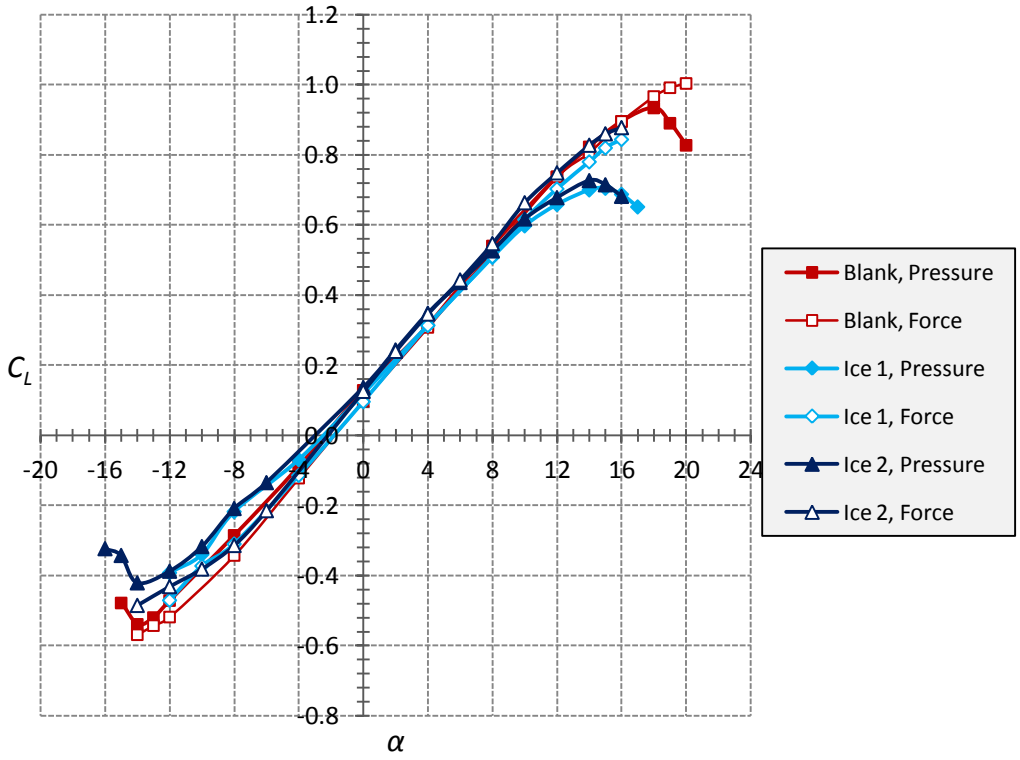

Figure 26 – Lift coefficient to angle of attack graph comparing the blank wing with the iced wings

Figure 26 compares the wind tunnel results for both the direct force method (white marker fill) and the pressure distribution method for the blank wing and the two types of ice. Ice 1 uses no plastelin to fill the upper gap while ice 2 does.

By first comparing the two methods for the iced wings, it's evident that the direct force method behaves the same way for the iced wings as it does for the blank wing. This gives an even stronger indication that the direct force measurements cannot measure the higher angles of attack. The results do seem to slightly indicate that ice 2 does have a lift curve which is shifted a bit upwards, creating higher lift. It appears that the plastelin had a minimum effect on the lift curve and no certain difference can be concluded between them. If more wind tunnel tests would have been made for the two iced wings, one might have been able to distinguish them. These results show that

the plastelin plays such a small part compared to the actual horn that it's almost negligible. Since the upper surface of the wing has the biggest impact on the lift force, one can also argue that adding the plastelin to the lower surface would have an even smaller effect on the results.

The most notable and important result by comparing the iced wings to the blank wing is that the stall angle has decreased from 18° for the blank wing, to 14° for the iced wings. That's a decrease of the stall angle of around 22%. The maximum lift force also decreased by the same percentage-wise amount. From 0° up to 8° the lift curves are more or less identical, but already at 8° the lift force starts to decrease compared to the blank wing.

The negative angles of attack are of less importance since civic aircraft descends slowly. What can be seen, though, is a wider spread of the curves, indicating that negative angles of attack are harder to measure. It appears that the iced wing curves do not "stall" earlier as the case with the positive angle of attack, but is instead shifted somewhat downwards. The negative lift force is thus slightly higher for the blank wing compared to the iced ones.

These results may be compared to previous made wind tunnel tests to verify its validity. One such experiment [6], compares the effects on the lift force for different types of ice with a blank wing. One general effect which may be seen from these tests, is that the ice (of all types) does not have any effect on the lift force on low to medium angles of attack. This behaviour can also be observed from the wind tunnel results in Figure 26. Another effect which is found both in the previous experiment [6] and the results shown in Figure 26, is that the lift force drastically decreases for the blank wing after the stall angle, in contrast to the iced wing where the decrease starts earlier and "lasts" longer. My hypothesis for this effect is that a blank wing either has a significant separation of flows which reattaches late to the surface or no separation of flow at all. For a wing with a horned-shaped ice on the other hand, a separation of air could happen at low angles of attack but will manage to reattach to the surface quickly thereafter.

In the previous study [6], the stall angle for the horned-shaped ice wing is as low as 8° while the blank stalls at 14°. This difference is much greater than the one observed in the wind tunnel tests in this project with this type of ice. This is not strange though, since the ice shape used in the previous experiment is different and has a greater horn covering the upper surface, while the tested horn-shape in this project is more profound on the lower surface. For positive angles of attack, a horn on the upper

surface has a bigger impact on the lift since an increase in angle of attack will strengthen the separation of flows effect.

In all, it appears like these previous wind tunnel tests [6] give a strong indication that the results gathered in this project could be correct.

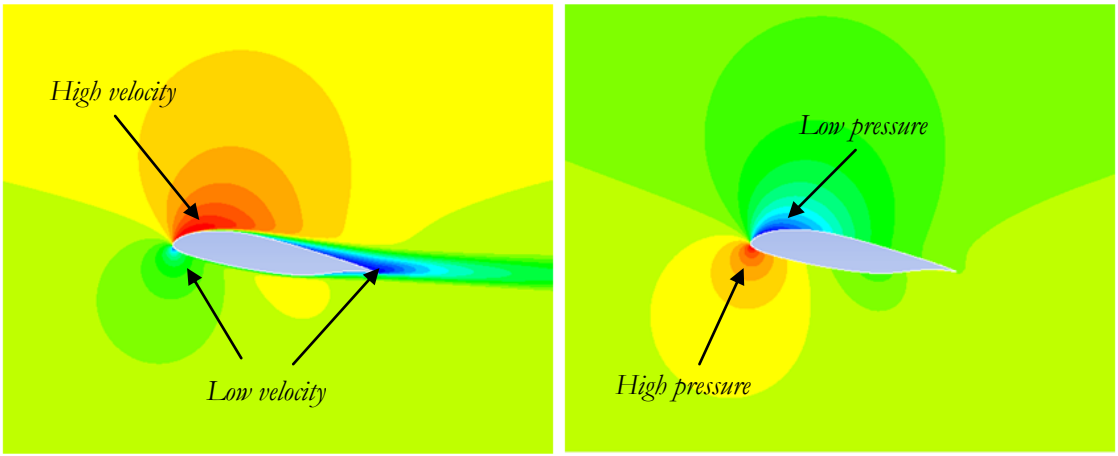

Figure 27 – Left side displays velocity while right side displays static pressure. α=8°

In Figure 27, contour results from the Fluent simulation of the blank wing are displayed. The left hand image displays the velocity profile around the blank airfoil. Yellow areas have the input velocity of 21.8 m/s, the maximum velocity is 32.8 m/s and is coloured red and the minimum velocity is 1.6 m/s and is coloured blue. One can see that the air is more or less completely still at the stagnation point at the tip and in the wake behind the airfoil. Note how the air travels much faster at the upper surface compared to the bottom and an increase in velocity results in a decrease in static pressure. This can clearly be seen on the right side where the static pressure of the airfoil is seen. Here, a red colour represents a higher pressure compared to the free stream pressure while a blue colour represents a lower pressure. Note how the colours are almost completely inverted compared to right except for the wake of slow moving air after the airfoil as seen on the left side. This wake would instead be visible for the dynamic pressure contours. By plotting the static pressure at the upper and lower surface, one would get curves similar to the blank curve in Figure 28.

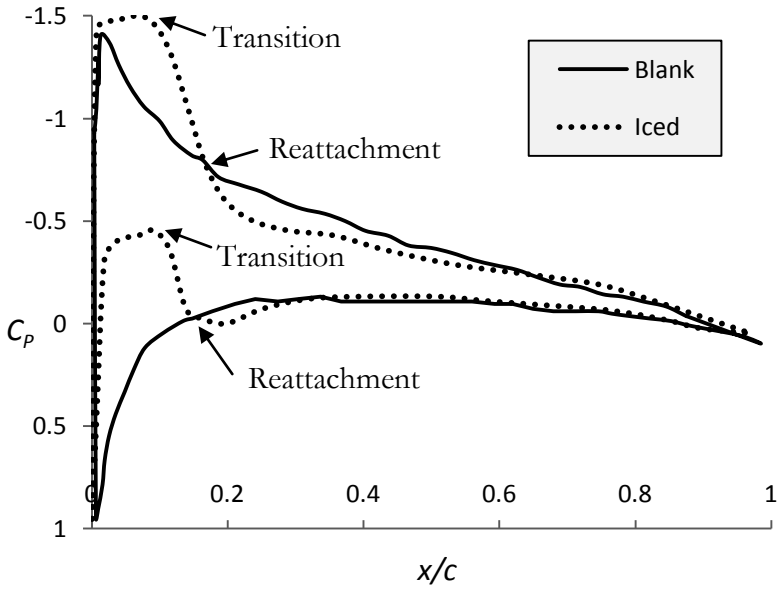

Figure 28 – Previous study comparing static pressure distributions of blank wing with iced wing at α=4 [5]

Figure 28 compares the static pressure distribution with an iced wing. The ice used is of a double-horned type displayed in Figure 6.

The areas marked as transition zones are zones where the flow is separated due to a high geometric discontinuity at the tip of the horns. In this area, the air is in turbulence and reversed flows are likely to occur. This causes the pressure to decrease, but as the air starts to reattach, the pressure will drastically increase (become more positive) until reattachment. This point is located where the ice curve intersects the blank wing curve, i.e. when they have the same pressure. After reattachment, the pressure slowly returns to the same values as for the blank wing.

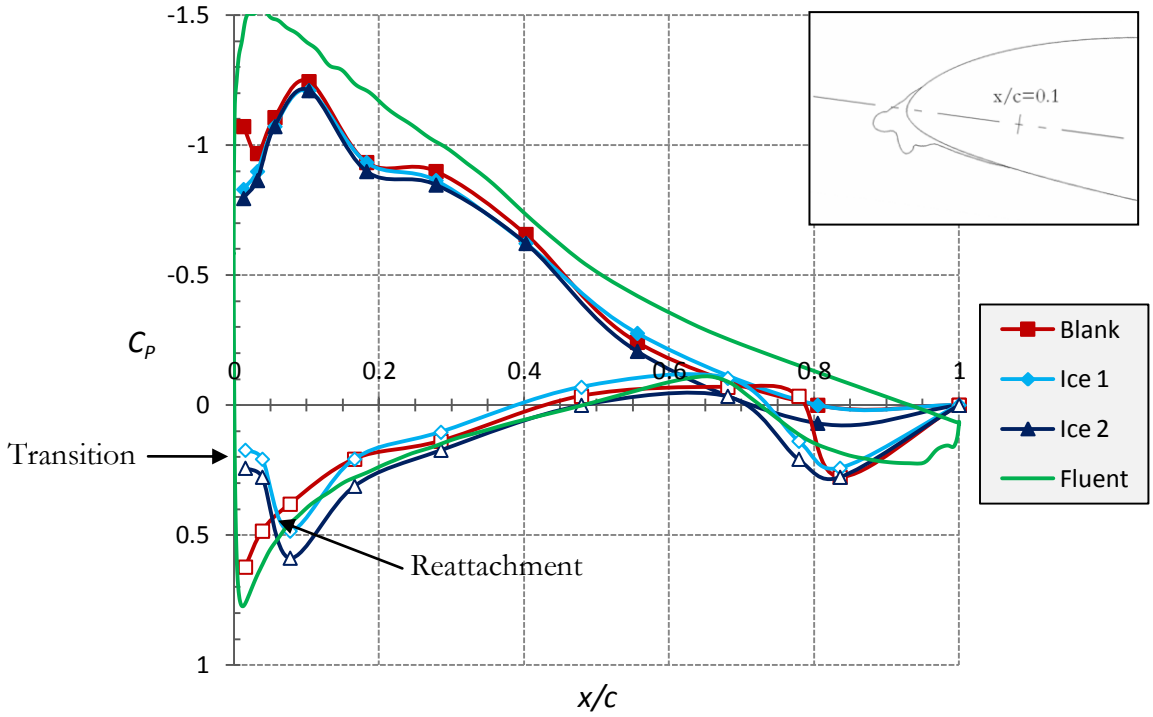

Figure 29 –Pressure distribution comparison at α=8°

Figure 29 displays the pressure distribution for the upper and lower (white marker filling) surfaces for the blank wing, the iced wings as well as the result from the Fluent simulation with the near wall treatment function for a blank wing for an angle of attack of 8°. Note that the y-axis is in reversed order so that the upper surface values are at the top for positive angles of attack. The point at x/c=1 belongs to neither upper nor lower surface and has not been measured, it is assumed that at the end of the wing the pressure is always zero. At the top right hand of the graph, the iced wing is illustrated with a corresponding angle of attack of 8°.

By comparing the blank wing with the result from Fluent, a rough match is seen where the general shapes are similar but while the Fluent curve is smooth, the wind tunnel test curve is a bit uneven on some locations. These locations are the first five points on the upper surface as well as the last two on the lower surface. The first one on top is believed to be an erroneous point since this value is higher than the second point for all other measured angle of attacks, as can be seen in Figure 23. It is believed that very small changes in the geometry have a big effect on the pressure distribution. At the location on the wing where sensor number five on top is positioned for example, one can see on the wing that the surface is slightly flattened. This means that the air has more space to spread, which reduces the velocity and thus increasing the pressure. Another reason for the variations could be that the tubes are not 100%

perpendicular to the surface of the wing, causing them to include some dynamic pressure.

By comparing the iced wings to the blank, one can clearly see the transition area at the lower surface where the pressure is lower. The air seems to reattach to the lower surface at around x/c=0.06, which seem reasonable for this angle of attack. By assuming that the first sensor on top of the blank wing is incorrectly measured, no transition layer can be seen on the upper surface. This also seems reasonable since this ice is positioned further down on the tip compared to the horn in Figure 6 for example.

By comparing ice 1 without plastelin to ice 2 with plastelin, one can see that the curves have the exact same shape. What's interesting though is that is seems like ice 2 has a higher pressure on the bottom side, shifting the curve downwards in the graph. This indicates that the velocity on the lower surface is lower for ice 2. This is hard to explain, but one theory is that the plastelin smoothen the airflow on the upper surface, causing more air to take this way and increasing the velocity on the upper surface while decreasing it on the lower. This theory would have been strengthened if the pressure was lower on the upper surface, something which is unfortunately not seen. Another explanation could simply be that the wind velocity of the wind tunnel somehow was changed between the tests. This does seem unlikely though, since the velocity was controlled before each run.

The static pressure distribution from the Fluent simulation without the near wall treatment is not printed. It follows the same shape as the one with the near wall treatment with the biggest difference being that the area is smaller without the near wall treatment and it fits better to the other curves.

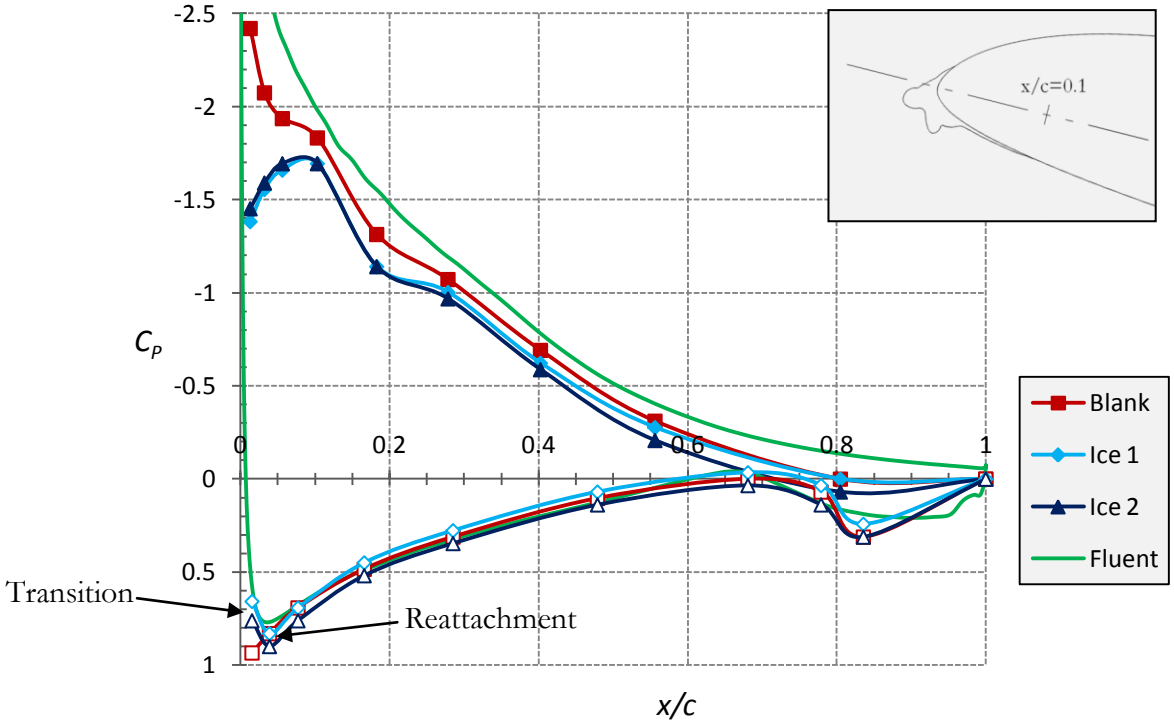

Figure 30 - Pressure distribution comparison at α=14°

Figure 30 shows the static pressure distribution for an angle of attack of 14°. As can be seen, the transition zone is smaller here and the air reattaches at x/c=0.025 compared to 0.060 at α=8°. This is reasonable since the ice is pointing downwards and as the angle of attack increases, more and more of the lower surface is exposed, limiting the transition zone. What's interesting in this graph is the three first points on the upper surface, where the pressure is higher for the iced wings compared to the blank one. This is because the ice acts like a ramp for the air which more or less lengthens the wing. This reduces the distance the air has to travel over the upper surface which in turn reduces its velocity and the lift force.

Note that points number five on top and the two last values on the bottom still have pressures either too high or too low compared to Fluent. This tells us that these points are unlikely to be an effect of faulty measurements.

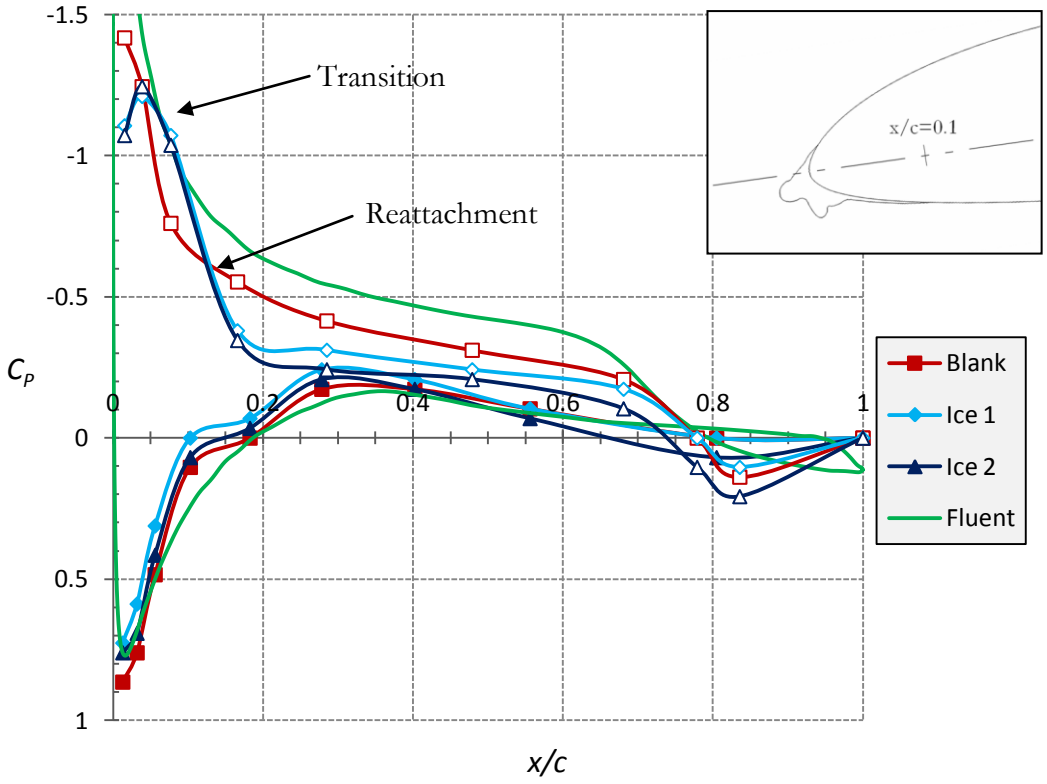

Figure 31 - Pressure distribution comparison at α=-8°

Figure 31 shows the static pressure distribution for the angle of attack -8°. The lower surface values now have a negative pressure while the upper surface values have a positive pressure, which means that the lift force is negative.

The upper surface curves for the blank and iced wings now follow the same shape without any bigger differences. This is not so strange, since the stagnation point is precisely above the ice layer, so that the air travelling on the upper surface doesn´t even "see" the ice. On the lower surface, one can clearly see a transition zone which stretches to x/c=0.125. Since the ice points downwards, the separation of flows become more severe for α=-8° compared to α=8°.

Another thing to note is that the lower values for ice 2 are still higher compared to ice 1, even for negative angles of attack. This more or less proves that the plastelin does affect the lift force and actually improves it to a certain degree.

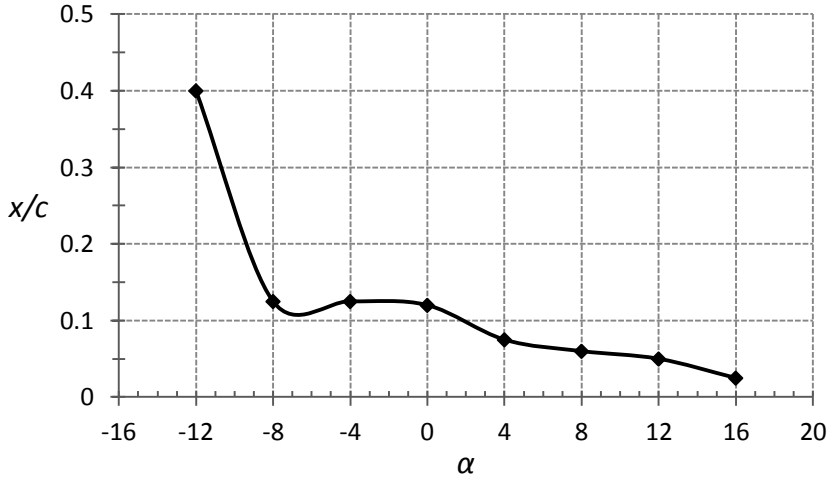

Figure 32 – Relation between reattachment points on lower surface and angle of attack

Figure 32 shows how the reattachment points at the lower surface changes depending on angle of attack. A pattern can be seen where the distance increases in a linear like manner from 16° down to -8°. At -12°, the distance raises drastically to almost half the length of the wing.

6.2 Drag force

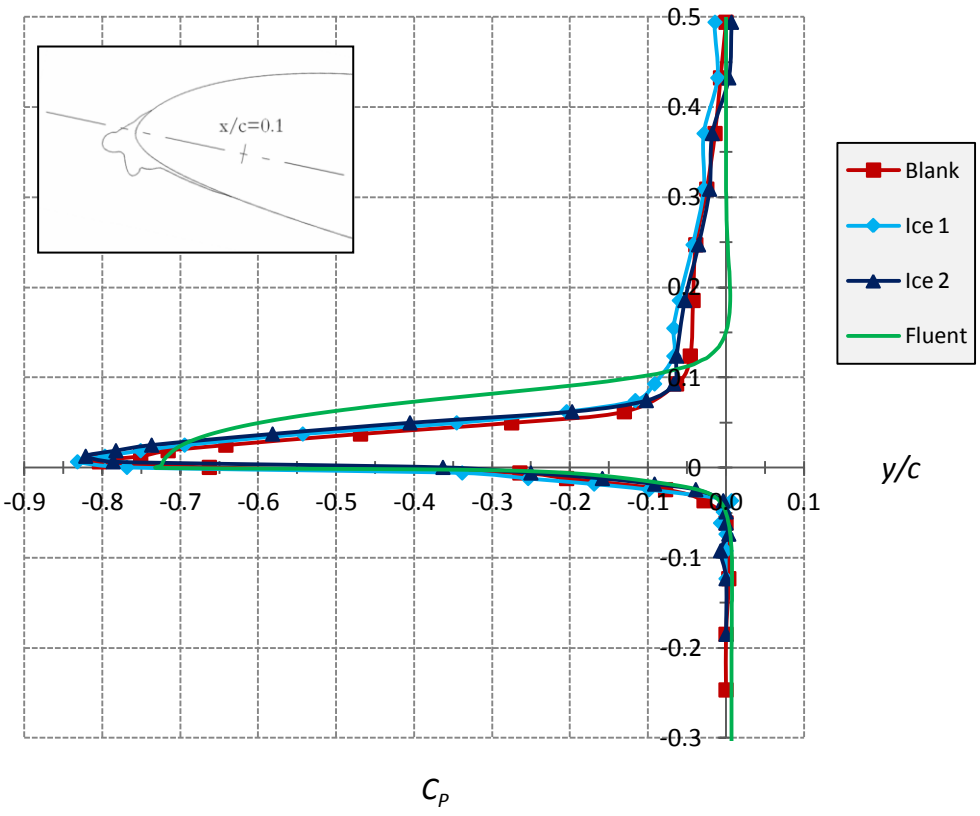

Figure 33 - Total pressure distribution at trailing edge at α=12°

Figure 33 shows the total pressure distribution at the wake after the airfoil at an angle of attack of 12°. The y-axis has been normalized by dividing the distance y from the trailing edge by the chord length c. Remember that in contrast to the static pressure, a high velocity increases the dynamic pressure and thus also the total pressure. A C_P value of zero indicates the pressure, and thus the velocity, of the free stream. A negative C_P value is hence an indication of a lower velocity compared to the free stream. The Fluent curve is from the simulation using the near wall treatment. The values for the blank wing and the iced wings are taken from measurements with the digital anemometer. These were also compared to values measured with the manometer and they proved to provide almost identical results. It proved difficult to get the exact values close to the trailing edge with the manometer though, since the alcohol level could have a range in pressure coefficient of up to approximately +/- 0.15. The manometer was chosen because of its ability to take samples and get an average where this problem was present.

Below the trailing edge, at negative y/c values, the match between Fluent and the blank wing is almost perfect. As the angle of attack is positive, the air flowing below the wing will be concentrated close to the trailing edge when released from the surface and its velocity is thus not that dependent on the shape of the lower surface. Above the trailing edge, the match is less convincing; the wind tunnel result show a lower minimum value as well as a longer upward distance where the wing has an effect on the total pressure. This should be an effect of the shape of the airfoil as discussed in the lift force results.

For this angle of attack, you can see no difference between ice 1 and ice 2 and by comparing these to the blank wing, only a very small difference can be seen. At first, it seems strange that the drag force is the same for an iced wing compared to a blank one. By observing the picture of the wing tip in Figure 33, one can see that the biggest horn is pointing directly towards the incoming air. This means that it will more or less serve as a cone and make the wing more streamlined which reduces the drag force. Of course, the lower, smaller, horn does not improve its aerodynamics and the drag would have been even lower without it. The differences between the ice types are almost non-existent. It is hard to tell the difference at the end of the wing when there is such a small difference at the front of the wing.

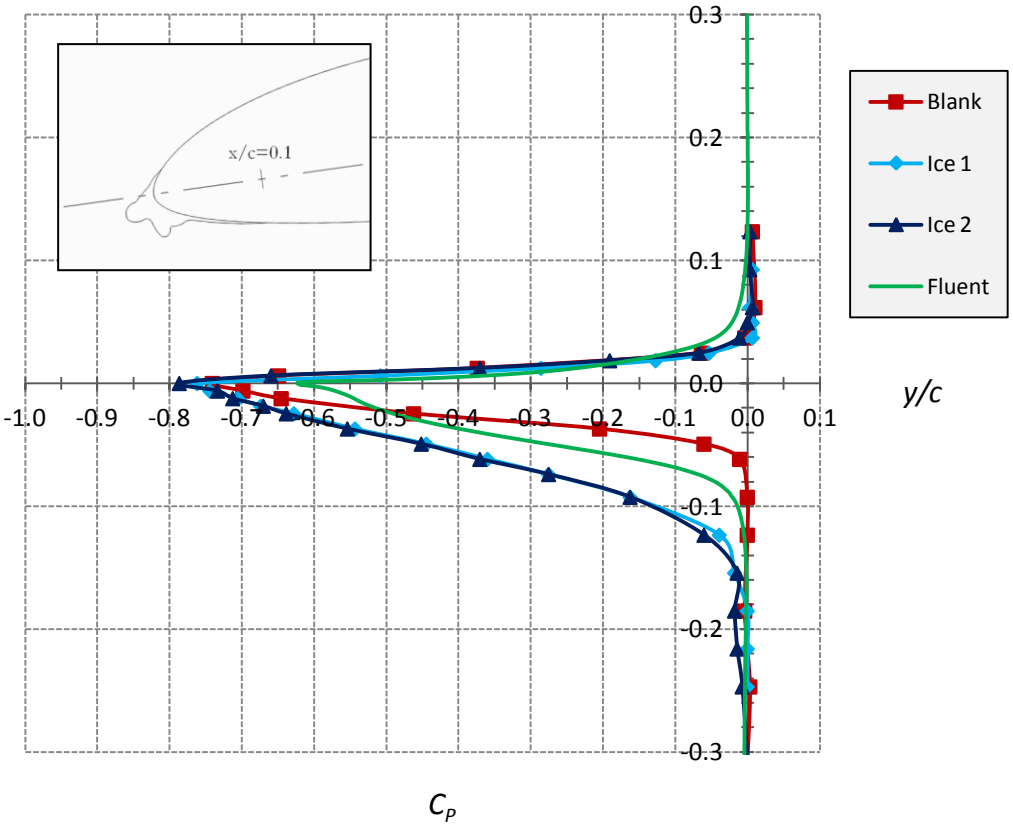

Figure 34 – Total pressure distribution at trailing edge at α=-8°

Figure 34 shows the total pressure distribution for a negative angle of attack of -8°. This time, Fluent matches the results closely for the blank wing above the trailing edge for the same reason as explained previously, that the air is more concentrated when leaving the upper surface (at a negative angle of attack). Also, the iced wings have the same shape as the blank wing above the trailing edge which further emphasizes this theory.

By comparing the two types of ice with the blank wing below the trailing edge, we see a clear increase in area (and thus drag force) for the iced wings, because of the separation of flows and the large transition zone. The air flowing on the lower surface of the blank wing, on the other hand, manages to stick to the surface all the way which can be seen by the fact that the curve is not far from being symmetric around the x-axis.

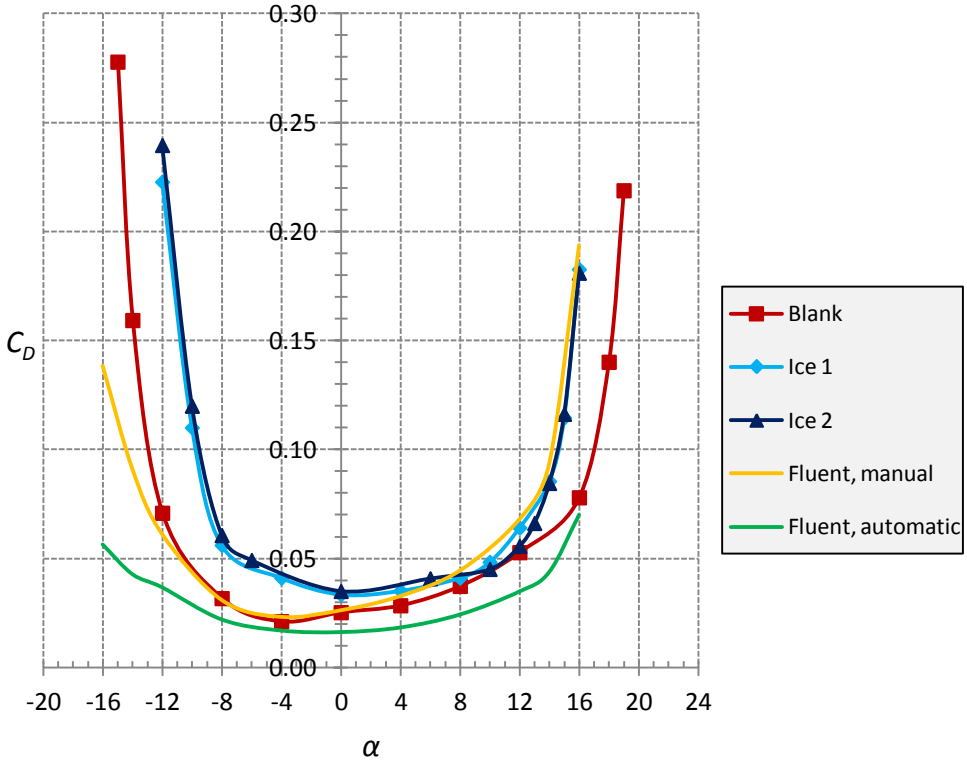

Figure 35 - Drag coefficient to angle of attack graph comparing wind tunnel results with Fluent results for a blank wing

Figure 35 shows the calculated drag coefficients for different angles of attack for the blank wing, the iced wings as well as the automatic and manual Fluent results with the near wall treatment.

Here, a problem is revealed in Fluent as the manual and automatic methods do not match each other. The manual method values are approximately 40% higher compared to those taken directly from Fluent using its automatic function. Either some factor in equation 20 is missing or something is wrong in the Fluent simulation. Based on the previous statement that the tested wing has a rough surface while Fluent does not, it seems most reasonable that the drag force from Fluent should be lower than the blank wing and that the automatic Fluent method therefore shows the most accurate results. By comparing the automatic Fluent method to the blank wing, they seem to more or less share the same shape except for the highest and lowest angle of attack. It is clear from both of these that the wing is asymmetric; a symmetric wing would have a symmetric drag force profile around the y-axis, which these graphs do not have.

The results from Fluent without using the near wall treatment are not displayed in the graph. The values from the automatic method without the near wall treatment are

approximately 3.8 times higher compared to the automatic method with the near wall treatment, which seem unreasonably high. Based on this fact, one can conclude that the near wall treatment gives a superior solution even though the lift force curve fit better, which could just have been a coincidence.

By comparing the iced wings to the blank wing, a clear difference is seen for most angles of attack. At an angle of attack of 0° for example, the drag increase for ice 1 compared to the blank wing is around 33%. This means that an airplane with this type of ice needs to compensate the increased drag with increased thrust from its motors to maintain the same velocity. The most noticeable differences are for the negative angles of attack, which seem logical based on previous arguments about the downward position of the ice. One can also see that the effect of the ice is not so severe around 10°, ice 2 has almost a lower drag here. This is also an effect of the position of the ice which acts like a streamlined cone at these angles of attack. After 12° though, the drag force rises considerably.

There are some smaller differences between the two types of ice. For negative angles of attack, ice 2 seems to have slightly higher drag but for positive angles of attack it seems to have slightly lower drag, especially around 12°. It is easy to imagine how the drag is lowered since the ice gets a smoother surface. Based on this theory, the drag should have been lower even for negative angles of attack. But the differences are small and can just as well have been an effect of a slightly different density or air velocity when performing the tests.

The direct force measurements are also missing from the graph. These were also eventually considered faulty because of the shape of the curve. From an angle of attack of 0° up to 16°, the lift curve was almost linear, a shape which does not fit to any previous study seen or to the Fluent results. At one occasion, three independent measurements were made by three different persons to conclude that it was not an effect of the human factor. The results were similar in shape and still almost linear but not identical, proving again that the method is unreliable. The theory is that something is wrong in the mechanics of the three component balance when measuring the drag.

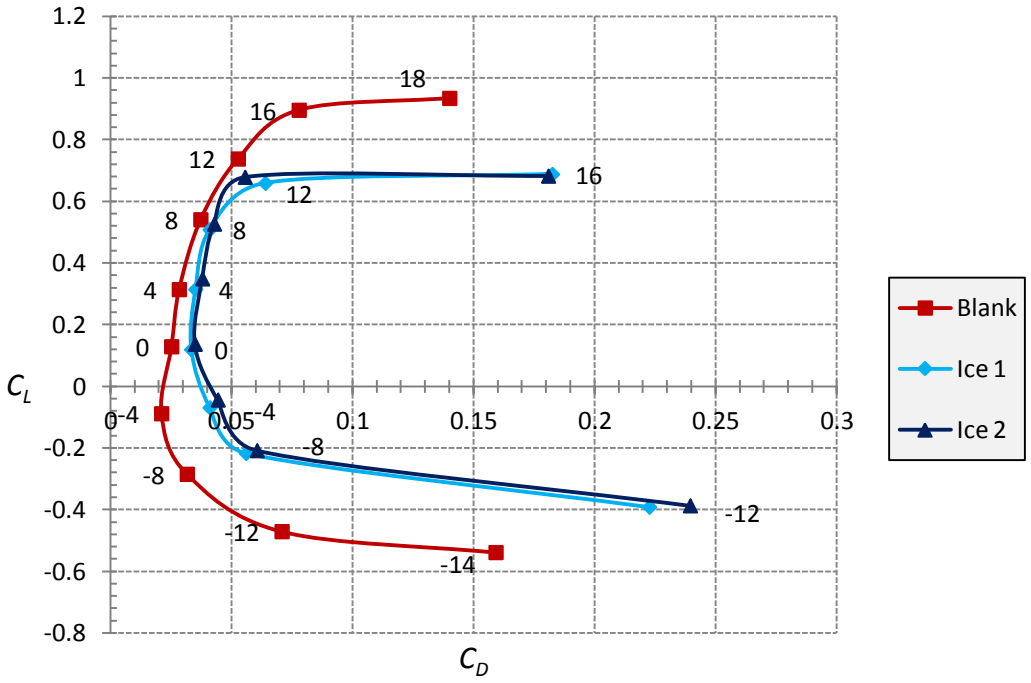

Figure 36 – Lift coefficient to drag coefficient graph for the wind tunnel results

The final graph, Figure 36, combines the lift and drag coefficient into one. The data labels indicate the angle of attack.

When developing a wing, you want the lift force to rise has high as possible with as little increase in drag as possible. In other words, the curve in this graph should go as steep upwards as possible when raising the angle of attack from 0°.

From 0° up to 12°, the curves are more or less parallel and have approximately the same lift force for each angle of attack. This tells us that the lift forces are similar in this area which has been shown previously. The graph also shows that for each level of lift force, the drag force is always higher for the iced wings. This means that the overall aerodynamic performance is always better for the blank wing when taking both the lift and drag forces into account. The interesting points in such graphs are the maximum lift before a significant increase in drag occurs. This point for the blank wing is clearly at 16° as the increase in drag from 16° to 18° is much higher compared to the increase from 12° to 16°. The maximum lift force occur at 18° for the blank wing, but to be able to achieve such a lift, a considerable increase in thrust needs to be applied to overcome the increase in drag force. Since more thrust means extra spent fuel and money, an airplane with this airfoil will unlikely go over an angle of attack of 16°. The same points for the iced wings are at 12°, 25% lower than the blank wing. As can be seen for the iced wings, the lift force is almost identical at 16° compared to at 12°, while the drag is three times higher.

By looking at the negative angles of attack, an even greater difference is seen, especially in the drag force. Here these points are positioned at -12° and -8° respectively, a decrease of 33%. This indicates that the drag is more severe at negative angles of attack which reflect previous theories about the shape and position of the ice.

6.3 Velocity, pressure and density studies

In addition to the wind tunnel tests, some smaller studies were made on the effect of changes in velocity, density and temperature.

As a pitot tube tests was conducted, the total pressure in the free stream seemed to constantly decrease during the course of the tests. The reason for this was not clear, so a study was made were the temperature was noted each time the free stream pressure was measured. The result from it is shown in Figure 37.

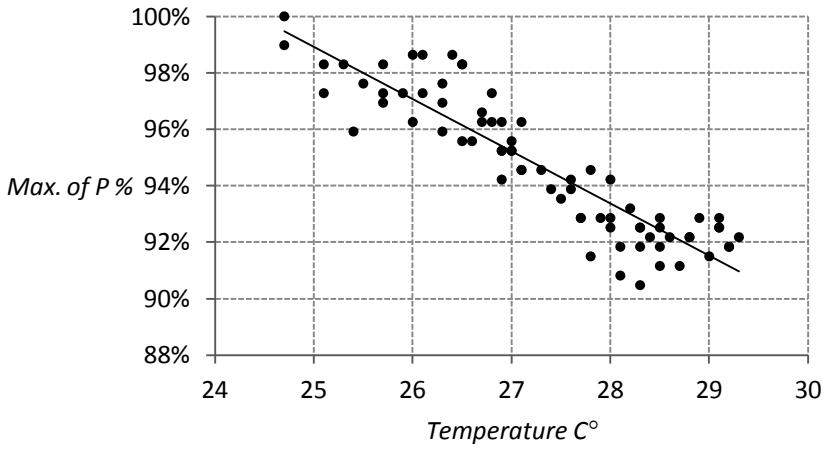

Figure 37 – Scatter plot showing the percentage loss in total pressure at different temperatures

The y-axis is defined as the pressure loss in percentage where the highest pressure value is considered as the first value with no pressure loss. The trendline shows that the pressure loss follows a linear pattern where the loss is approximately 1.8% for each raise of 1 C°. Both the degree to which the wind tunnel heated up the room and the corresponding decrease in total pressure were higher than expected and are interesting findings. The decrease in pressure is not seen in the results of the drag measurements since the pressure in the free stream was updated for each angle of attack.

Another interesting aspect to control was how well the wind tunnel was able to maintain the set velocity. 20 values were measured independent of each other and each was measured using the time-average function of the anemometer. The mean value, μ, turned out to be 21.889 m/s with a spread, σ, of 0.225 m/s. 2/3 of the values are in the interval of 21.665 m/s to 22.114 m/s. This spread is a bit bigger than first expected. Let's say that you use a wind velocity that is equal to: 22.114-21.665 = 0.449 m/s away from the value you use in the calculations, the fault you make then is 4.2%. Assuming that it´s unlikely to measure it that incorrectly, one can argue that a realistic value could be around 1-2% if the velocity is measured carelessly. Even though you do measure it carefully, the velocity of the wind tunnel could still change after that. This span in velocity is difficult to apply to the calculations but is something to keep in mind.

As can be seen in Figure 37, the temperature may change drastically during an experiment run. As the temperature changes, so does the density of the air which is used in the calculation of the lift and drag coefficients. If you use a density corresponding to a temperature which is 5 C° away from the actual value, the fault you make is 1.7%. This is small in comparison to the velocity, even though a 5 C° difference is high. This is because while the velocity is squared in the calculations, the density is halved.

Assuming constant density and velocity in tests like these are easily made. Apparently, these factors shouldn´t be taken that lightly since it can have an effect to some degree. Hopefully, these factors didn´t have a major effect on the results on this project work.

7 Conclusions

The main goals of creating an ice layer, applying it to a wing and make comparisons using a wind tunnel have all been achieved. The process of manufacturing the ice layer was problematic, but successful in achieving the target specifications. It was robust and did not break during tests, it had accurate shape and position and it did not damage the wing. Even though it was not an explicit goal, the method of manufacturing an ice layer with the software and equipment available at the university could be considered a result in itself. By following the methods in this report, another person should be able to generate other types of ice layers for new wind tunnel tests.

The hypothesis before conducting the wind tunnel experiments was that the maximum possible lift force would decrease upon icing. It also did by approximately 22% which is a reasonable result based on the position and shape of the ice in comparison to another study [6]. The drag also increased for most angles of attack, as expected. At an angle of attack of 0° for example, the increase in drag force is around 33% higher for the iced wing compared to the blank wing. The drag is higher at negative angles of attack but less severe for positive ones. An interesting result is that the drag was almost unaffected for angles of around 10°, a possibility that was not considered before the experiments started. Another conclusion is that the static pressure distribution is very sensitive to even the slightest variations in the geometry of the wing surface. These variations are barely visible but are still seen in the results.

From the completed experiments, it is clear that a horn-shaped type of ice has a noticeable effect on the aerodynamic performance of a wing. It is not hard to imagine that in-flight icing is a big threat to the safety of aviation and something that needs to be dealt with further. If this ice would be left to increase more in size, the effects could be devastating.

The Fluent simulations proved to be difficult and did not provide as good results as was hoped for. There are similarities between the Fluent results and the results from the wind tunnel tests, but could have been more convincing. Since the wing replica does not fully match the wing model in Fluent regarding shape and roughness, it´s hard to determine if the solution in Fluent is correct or not.

7.1 Reflections

The development of the ice layer was made as a modified product development process [13]. This methodology was followed as well as possible but was difficult for a couple of reasons. There was no real costumer for this project, which means that no interviews could be made and setting the target specifications was hard. Another issue was that the product was not similar to any other product available. Therefore, it was hard to make any external comparisons. The pros and cons lists and the concept scoring matrix were possible to perform and proved to be helpful for some problems.

The ice layer was eventually finished after plenty of problems. The most time consuming obstacle was the fact that the ice did not properly fit to the wing. It was first assumed that the wing had the correct shape and therefore the theory for a long time was that the shape of the ice layer was faulty. A lot of time would have been saved if the shape of the airfoil was questioned from the start. It was also hard to find the best solution for how to mount the ice to the wing, since no knowledge in the area existed. A secondary target from the start was to simulate, create and test more types of ice. Unfortunately, many steps took longer than expected and no time was left to make any additional ice layers.

Another smaller issue in the process was that the CAD models needed to be created and handled in Pro/Engineer, a software which was unfamiliar before the project. It was also in German which made it even more difficult. The method of transferring the coordinates of the ice into the software was complicated even though the final solution proved to be simple.

Once the wind tunnel tests started, it was wrongly believed that fewer problems would occur. The main issue, as mentioned in the results, was that the direct force measurement of the drag was so different from the pressure method. A lot of work was invested in this issue, the micrometer screw was exchanged for example and tests were made on the spring coefficient of the spring measuring the drag. None helped and after comparison with results from Fluent and other studies, it was concluded that something must be wrong in the mechanics of the three component balance.

Simulations in Fluent were not originally planned to be done in this project but were performed anyway to have something to compare to the wind tunnel results. Luckily, a simulation of the correct airfoil had already been made by my supervisor, Mr Gilbert, and was used with some smaller adjustments. Fluent is generally problematic, since it´s hard to know if you have the correct solution. It was joyful to see how well the lift force curve matched to the results from the blank wing but when proceeding with comparisons to drag it was evident that the solution was not correct. With the

near wall treatment, which was found late in the project, the drag results got better but it also affected the lift force curve which was unfortunate.

I believe that this project has been a fun and challenging experience. I have learned lots about aerodynamics, Fluent and how to perform wind tunnel measurements and calculations. I have made personal progress and I believe that I have learnt to work and to think more like an engineer; analytically and systematically. I have also learnt that one should never assume that something is correct just because someone tells you that it´s correct. Always question its reliability. I believe that it has been a good experience to have worked with people from a different culture than your own, I think that will give me a wider scope of thinking.

7.2 Future work

This project has opened up an opportunity to much further work at the University of Applied Sciences in Kaiserslautern. Since a method in creating these ice layers has been developed, it´s now possible to create additional types of ice to be tested in the wind tunnel. Of course, a lot of work is required to simulate the actual shapes of the types of ice for this airfoil but this can hopefully be done with Mr. Gilbert's ice accretion code. Work also needs to be put into figuring out what types of ice to be tested. Maybe one of each of the four types; roughness, horn ice, streamwise ice and spanwise ridge could be created or variations of each single type. For the horn-shaped ice, the position of it is interesting since it changes the transition areas for example.

More work can also be done in Fluent to either confirm that the model presented in this report is correct, or to find out what is missing and correct this.

8 Bibliography

1. **Mitchell, Mark.** *Digitizer Sourceforge.* [Online] April 2009. http://digitizer.sourceforge.net/.

2. **ANSYS.** *FLUENT.* [Online] [Cited: 10 July 2011.] http://www.ansys.com/Products/Simulation+Technology/Fluid+Dynamics/ANSYS+FLUENT.

3. **NASA.** LEWICE. [Online] [Cited: 10 July 2011.] http://icebox.grc.nasa.gov/design/lewice.html.

4. **PTC.** *Pro/Engineer.* [Online] [Cited: 10 July 2011.] http://www.ptc.com/products/creo/parametric.

5. *Iced-Airfoil Dynamics.* **Bragg, M.B., Broeren, A.P. and Blumenthal, L.A.**

6. *Airfoil Ice-Accreation Aerodynamics Simulation.* **Bragg, M., et al.**

7. *Update to the NASA Lewis Ice Accretion Code LEWICE.* **Wright, William B.** http://ntrs.nasa.gov/archive/nasa/casi.ntrs.nasa.gov/19950007881_1995107881.pdf.

8. **North Carolina Department of Environment and Natural Resources.** Meterological Paramenter. [Online] [Cited: 10 July 2011.] http://www.ncair.org/monitor/real/parameters.shtml.

9. **NASA.** Aerodynamics Index. [Online] [Cited: 25 August 2011.] http://www.grc.nasa.gov/WWW/K-12/airplane/short.html.

10. **Anderson, John Jr.** *Fundamentals of Aerodynamics.* s.l. : McGraw-Hill, 1984.

11. **Nave, R.** Bernoulli or Newton's Laws for Lift? [Online] http://hyperphysics.phy-astr.gsu.edu/hbase/fluids/airfoil.html.

12. **Steuernagle, John, Roy, Kathleen and Wright, David.** *Aircraft Icing.* [Online] http://www.aopa.org/asf/publications/sa11.pdf.

13. **Ulrich, Karl T. and Eppinger, Steven D.** *Product Design and Development.* [ed.] International. s.l. : McGRAW HILL, 2008.

14. *Internal document.* **Gilbert, Norbert.** University of Applied Sciences.

15. **Ansys.** Fluent 6.3 Documentation. [Online] Mainly chapter 12.10.4.

Pros and Cons lists and Concept Scoring Matrix

Problem: Positioning the ice layer on the precise spot on the wing

Solution	Pros	Cons
End Profile At the end of the ice layer, create a thin airfoil profile connected to it. Glue this surface to the end of the wing.	■ This creates a profile of the thinnest parts which can be used when creating them ■ Easy and fast to mount it to the wing ■ There is no need to remove the extra support surface ■ If created with small "flaps" at the back the ice could be snapped onto the wing which will result in less use of glue	■ The sides of the wing needs to be glued ■ Might be hard to remove ■ If using flaps, the result may be biased. Needs to be investigated ■ It needs to be investigated whether the extra length has any effects on the results
Negative Form Create a negative form of the tip of the wing and the ice layer. It´s dimension should be a bit bigger, maybe around 0,1 mm, to ensure a good fit.	■ Its possible to ensure good fit along the entire wing by sliding the negative form along it ■ If there is any uneven surfaces on the ice layer it will be found and can be corrected	■ Will require some time to get the correct dimensions on the negative form ■ Will take time to create and requires a lot of material ■ If there is any uneven surfaces on the wing it might create a problem
Curvature Extension Create a thin extension at the end of the ice layer which follows the curvature of the wing. It should be around 1 cm in width and maybe half the depth of the wing. The ice layer is positioned with this as a guideline and once in place it is carefully removed with a sharp knife.	■ Easy and fast to mount it to the wing	■ May damage the wing ■ May be difficult to remove without changing the position of the ice layer
3D Measurement and putty Mount the ice layer to the wing using putty on the edges. Use the 3D measurement machine to control the position and then make small adjustments and repeat until the position is correct.	■ No need for creating extra support material or change the CAD file ■ If it's easy to place it correctly from the start it could be a very fast method	■ If it's hard to place it correctly from the start it could be a very time consuming method ■ Ice layer may move slightly after its mounted

Wing Extrusion In the CAD model of the ice layer, create a small extrusion to indicate where the tip of the wing should be. Match this indication to the actual wing tip when mounting it.	■ Simple solution	■ Bad precision ■ Hard to change position once placed

Problem: Positioning the ice layer on the precise spot on the wing

		End Profile		Negative Form		Curvature Extension		3D Measurement and putty		Wing Extrusion	
Selection Criteria	Weight	Rating	Weighted Score	Rating	Weighted Score	Rating	Weighted Score	Rating	Weighted Score	Rating	Weighted Score
End Precision	0.21	**5**	1.04	4	0.83	4	0.83	4	0.83	1	0.21
Easy to apply	0.10	4	0.42	3	0.31	3	0.31	1	0.10	3	0.31
Easy to remove	0.06	3	0.19	3	0.19	3	0.19	3	0.19	3	0.19
Does not damage the wing	0.15	3	0.44	**5**	0.73	4	0.58	**5**	0.73	**5**	0.73
Precision in 3rd direction	0.21	3	0.63	4	0.83	3	0.63	3	0.63	3	0.63
Durability during testing	0.08	**5**	0.42	3	0.25	3	0.25	3	0.25	3	0.25
Unbiased readings	0.19	3	0.56	3	0.56	3	0.56	3	0.56	3	0.56
Total Score		3.69		3.71		3.35		3.29		2.88	
Rank		2		1		3		4		5	
Continue?		Combine		Combine		No		No		No	

Problem: How to create the thinnest parts of the ice layer

Solution	**Pros**	**Cons**	**Score (1-5)**
Plastelin Do not create the layers with thickness < 1mm and manually apply "plastelin" to the thinnest parts. Create a negative form in metal which is used to achieve the correct shape	■ Durable ■ With a negative metal form it's possible to achieve a good shape along the entire wing ■ Easy to remove ■ Very thin films can be created	■ Hard to apply ■ Time consuming	**4**
Putty Do not create the layers with thickness < 1mm and manually apply removable adhesive putty on the thinnest parts	■ Relatively easy to apply ■ Possible to create a smooth surface ■ Possible to make very thin layers	■ Small risk of creating damages to the wing ■ May take a long time to achieve a good result	**3**
Grinding Grind down the thinnest layers with a drill	■ No thickness variations across the third direction	■ Time consuming ■ Hard to make smooth transitions in x-direction ■ Risk of destroying the part	**2**
Ignore Do not create the layers with thickness < 1mm and assume that it won´t affect the results in a major way	■ Easy ■ Saves time once validated	■ Need to investigate the effects of such assumption ■ Risk of untrustworthy results ■ May be harder to position ice layer correctly	**2**